



The Subantarctic lithospheric mantle

Guillaume Delpech, James M Scott, Michel Grégoire, Bertrand N. Moine, Dongxu Li, Jingao Liu, D. Graham Graham Pearson, Quinten H A van Der Meer, Tod E Waight, Gilbert Michon, et al.

► To cite this version:

Guillaume Delpech, James M Scott, Michel Grégoire, Bertrand N. Moine, Dongxu Li, et al.. The Subantarctic lithospheric mantle. The Geochemistry and Geophysics of the Antarctic Mantle, pp.M56-2020-13, 2021, 10.1144/M56-2020-13 . hal-03266963

HAL Id: hal-03266963

<https://hal.science/hal-03266963>

Submitted on 22 Jun 2021

HAL is a multi-disciplinary open access archive for the deposit and dissemination of scientific research documents, whether they are published or not. The documents may come from teaching and research institutions in France or abroad, or from public or private research centers.

L'archive ouverte pluridisciplinaire **HAL**, est destinée au dépôt et à la diffusion de documents scientifiques de niveau recherche, publiés ou non, émanant des établissements d'enseignement et de recherche français ou étrangers, des laboratoires publics ou privés.

Accepted Manuscript

Geological Society, London, Memoirs

The Subantarctic lithospheric mantle

Guillaume Delpech, James M. Scott, Michel Grégoire, Bertrand Moine, Dongxu Li, Jingao Liu, D. Graham Pearson, Quinten H. A. van der Meer, Tod E. Waight, Gilbert Michon, Damien Guillaume, Suzanne Y. O'Reilly, Jean-Yves Cottin & André Giret

DOI: <https://doi.org/10.1144/M56-2020-13>

To access the most recent version of this article, please click the DOI URL in the line above. When citing this article please include the above DOI.

Received 9 April 2020

Revised 11 September 2020

Accepted 13 September 2020

© 2021 The Author(s). Published by The Geological Society of London. All rights reserved. For permissions: <http://www.geolsoc.org.uk/permissions>. Publishing disclaimer: www.geolsoc.org.uk/pub_ethics

Supplementary material at <https://doi.org/10.6084/m9.figshare.c.5424956>

Manuscript version: Accepted Manuscript

This is a PDF of an unedited manuscript that has been accepted for publication. The manuscript will undergo copyediting, typesetting and correction before it is published in its final form. Please note that during the production process errors may be discovered which could affect the content, and all legal disclaimers that apply to the book series pertain.

Although reasonable efforts have been made to obtain all necessary permissions from third parties to include their copyrighted content within this article, their full citation and copyright line may not be present in this Accepted Manuscript version. Before using any content from this article, please refer to the Version of Record once published for full citation and copyright details, as permissions may be required.

The Subantarctic lithospheric mantle

Guillaume Delpech¹, James M. Scott², Michel Grégoire³, Bertrand Moine⁴, Dongxu Li⁵, Jingao Liu⁵, D. Graham Pearson⁶, Quinten H.A. van der Meer⁷, Tod E. Waight⁸, Gilbert Michon⁴, Damien Guillaume⁴, Suzanne Y. O'Reilly⁹, Jean-Yves Cottin⁴, André Giret⁴

1, Université Paris-Saclay, CNRS, GEOPS, 91405, Orsay, France

2, Department of Geology, University of Otago, Dunedin 9054, New Zealand

3, Géosciences Environnement Toulouse, OMP; CNRS-CNES-IRD-Toulouse III University, France

4, Laboratoire Magmas et Volcans; CNRS-IRD-St Etienne and Clermont-Ferrand Universities, St Etienne, France

5, State Key Laboratory of Geological Processes and Mineral Resources, China University of Geosciences, Beijing 100083, China

6 Department of Earth and Atmospheric Sciences, University of Alberta, Edmonton, Alberta T6G 2E3, Canada

7, Nordic Volcanological Center, Institute of Earth Sciences, University of Iceland, Sturlugata 7, 101 Reykjavík, Iceland

8, Department of Geosciences and Natural Resource Management (Geology Section), Copenhagen University, Øster Voldgade 10, 1350 Copenhagen K, Denmark

9, Centre of Excellence for Core to Crust Fluid Systems and GEMOC National Key Centre, Earth and Planetary Sciences, Macquarie University, Australia

ABSTRACT

We present a summary of peridotite in the Subantarctic (46 to 60°S) surrounding the Antarctic Plate. Peridotite xenoliths occur on Kerguelen and Auckland islands. Kerguelen islands are underlain by a plume whereas the Auckland Islands are part of continental Zealandia, which is a Gondwana-rifted fragment. Small amounts of serpentinised peridotite has been dredged from fracture zones on the Southeast Indian, Southwest Indian, and Pacific Antarctic Ridge, and represents upwelled asthenosphere accreted to form lithosphere. Supra-subduction zone peridotite has been collected from two locations on the Sandwich Plate. Peridotites from most Subantarctic occurrences are moderately to highly depleted, and many show signs of subsequent metasomatic enrichment. Os isotopes indicate that the Subantarctic continental and oceanic lithospheric mantle contains ancient fragments that underwent depletion long before formation of the overlying crust.

‘Supplementary material: [description of material, photomicrographs, mineralogical and geochemical data] is available at’.

1. INTRODUCTION

The Subantarctic is an area circumnavigating Earth between 46°S and 60°S (**Fig. 1**). It encompasses seven major tectonic plates (Antarctic, Australian, Pacific, Scotia, South Sandwich, South American and African) but, with the exception of the southern tip of South America and the southern portion of New Zealand, only small island groups breach the ocean surfaces. The islands, referred to as Subantarctic islands, form 13 groups that range in area from 7215 km² (Kerguelen) to 1.4 km² (Bounty) (**Fig. 1; Table 1**); all are difficult to access and remote, and none have a permanent human population. The island groups are typically intraplate volcanoes (Weaver et al., 1987; Barling and Goldstein, 1994; Mahoney et al. 1996; Giret et al., 1997; Quilty and Wheller, 2000; Leat et al. 2003; Le Roux et al. 2012; Scott and Turnbull 2019) with the exception of the Zealandia granite-dominated Snares and Bounty island groups (e.g., Scott and Turnbull 2019), and Macquarie Island, which is a slice of exhumed oceanic lithosphere (Kamenetsky et al. 2000; Varne et al. 2000).

In this contribution, we summarise the characteristics of the Subantarctic lithospheric mantle in the Southern Ocean and the southern Atlantic and Indian oceans, as known from mantle peridotite. As will be discussed below, peridotite xenoliths have been found on three Subantarctic Island groups: Kerguelen and Heard islands in the southern Indian Ocean, and Auckland island in the Southern Ocean. Exhumed abyssal peridotite is exposed on Macquarie Island in the Southern Ocean, and has been dredged from the Southwest and Southeast Indian and America-Atlantic ridges (**Fig. 1**), and supra-subduction zone peridotite has been dredged and drilled from the South Sandwich arc in the Atlantic Ocean. Our synthesis of the Subantarctic lithospheric mantle peridotite is presented in three domains: the Indian Ocean, the Southern Ocean and the Atlantic Ocean. A very brief review of some locations was given in Nixon (1987).

Since the oldest oceanic crust surrounding Antarctica is Cretaceous, the fragmentation of Australia, India, Zealandia, South America and Africa from Antarctica has led to dispersion of continental lithospheres and formation of intervening areas of oceanic lithosphere by asthenosphere decompression. Therefore, the composition and evolution of rare fragments of peridotite from under the southern portions of the Indian, Southern and Atlantic oceans provides rare insight into the evolution of fragments of dispersed Gondwana lithosphere, as well as the upwelled and accreted

mantle that formerly resided deep beneath the continents but now represents the intervening oceanic lithosphere.

2.1 SUBANTARCTIC MANTLE UNDER THE SOUTHERN INDIAN OCEAN

The ~7200 km² Kerguelen archipelago is the main island of the French Subantarctic island group (Terres Australes et Antarctiques Françaises; TAAF) in the Indian Ocean and is located on the northern part of the submerged Kerguelen-Heard oceanic plateau (**Fig. 2A**). This plateau is the second largest oceanic Large Igneous Province in the world (25 × 10⁶ km³) after the Ontong Java Plateau (Coffin & Eldhom, 1993). The Kerguelen archipelago is the only place where mantle xenoliths have been intensively studied in the southern Indian Ocean. Rare peridotite xenoliths occur on Heard Island (O'Reilly, pers. observations) but no data are currently available, and the dunite xenoliths reported from Crozet by Nixon (1987) are actually igneous cumulates (**Table 1**).

The Kerguelen-Heard plateau formed in response to Kerguelen plume magmatism, which is closely linked with the Gondwana breakup in the southern hemisphere that started 120 Ma ago (Coffin et al., 2002). According to geodynamic reconstructions and geochemical investigations (e.g., Royer & Coffin, 1992), the archipelago originated from interaction between the Kerguelen plume and the South East Indian Ridge about 40 Ma. The ridge then progressively moved away from the hotspot, leaving the plume in its oceanic intraplate position since ~25 Ma. The majority (80 to 85%) of the sub-aerial surface of the Kerguelen archipelago is covered by flood basalts that erupted 30 to 25 Ma and reach > 1000 m thick in places (Giret, 1993). However, small volume disseminated Quaternary volcanic centres point to ongoing but limited magmatic activity. The volcanic rocks comprise an early tholeiitic-transitional series followed by alkaline and then highly alkaline magmas (Doucet et al., 2002, 2005; Frey et al., 2000; Gautier et al., 1990; Weis et al., 1993; Yang et al., 1998). The rest of the sub-aerial rocks are made of plutonic rock types (~15%, comprising gabbros, syenites, Qz-monzonites and rare granites) associated with the volcanic systems (Lameyre et al., 1976; Dosso et al., 1979; Giret, 1983; Scoates et al., 2008) and sedimentary rocks formed by fluvio-glacial erosion.

2.2 Kerguelen peridotite xenolith characterisation

The earliest descriptions and collection of mantle xenoliths from Kerguelen were made by Aubert de la Rue and Edwards, respectively, in 1932 and 1938. Although xenoliths were subsequently mentioned regularly in publications (Talbot et al., 1963; Nougier, 1970; McBirney and Aoki, 1973;

Giret, 1983; Gautier, 1987; Leyrit, 1992), systematic study only really began in the early 90's during the Kerguelen cartographic programs initiated by André Giret and the TAAF. The results of these studies make Kerguelen one of the best studied off-craton mantle xenolith occurrences on Earth (Grégoire et al., 1992, 1994, 1995, 1996, 1997, 1998, 2000a-b, 2001; Mattielli et al., 1996, 1999; Schiano et al., 1994; Valbracht et al., 1996; Moine et al., 2000, 2001, 2004; Lorand et al., 2004; Delpech et al., 2004, 2012; Bascou et al., 2008; Wasilewski et al., 2017). There are at least 22 mantle xenolith localities (**Fig. 2B**), all occurring within dykes, lava flows and breccia pipes of the youngest and most alkaline volcanic rocks. Most xenoliths have sub-rounded shapes, with sizes ranging up to 60 cm in diameter. Grégoire (1994) and Grégoire et al. (1995) subdivided Kerguelen xenoliths into two main groups: Type-I and Type-II. The type-I xenoliths comprise spinel-bearing harzburgite (30%), dunite (10%) and associated composite rocks. These are commonly very fresh, except a group of moderately serpentinised harzburgites from Lac Michèle (Wasilewski et al., 2017). The type-II xenoliths (50%) are metacumulates (peridotites, pyroxenites and metagabbros) recrystallized in the P-T conditions of the lower crust and upper mantle. The remaining 10% are hornblendites, biotitites and amphibole- or biotite-bearing clinopyroxenites with typical cumulative textures. In this contribution, we discuss published and new data for Type I xenoliths.

The Type I spinel-bearing harzburgite xenoliths mostly have coarse-grained textures (**Supplementary Table 1 and Supplementary Fig. 1**) that locally grade into porphyroclastic textures comprising fine-grained mosaics of olivine and orthopyroxene neoblasts surrounding elongate porphyroclasts. These common "protogranular" harzburgites consist mostly of olivine and orthopyroxene with low modal contents of clinopyroxene (< 5 %) and spinel. Accessory phlogopite, amphibole, apatite, carbonate and feldspar occur in some samples. Although Cr-diopside is the main clinopyroxene (Grégoire, 1994), many harzburgites also display "poikilitic" Mg-augite crystals with magmatic twins and/or as spongy rims surrounding orthopyroxene, olivine and spinel, sometimes associated with phlogopite and more rarely with amphibole and apatite (**Supplementary Fig. 1B, 1C**). Poikilitic peridotites are often cut by veins of amphibole (pargasite) and/or phlogopite (**Supplementary Fig. 1D**). These two main types of peridotite, protogranular and poikilitic, are observed in almost all the xenolith localities among the archipelago but the protogranular samples always occur in greater abundance. Very rare clinopyroxene-poor lherzolites are present (Valbracht et al., 1996; Grégoire et al., 2000; Schiano et al., 1994; Mattielli et al., 1996) and they are considered to

belong to the poikilitic peridotite group. The third sub-group within the Type 1 Kerguelen peridotites - dunite - essentially consists of olivine with minor spinel and clinopyroxene. These rocks show equigranular or inequigranular textures (**Supplementary Fig. 1E, 1F**). The spinel and clinopyroxene modal contents are sometimes more abundant than in harzburgites (up to 3.5% and 7%, respectively) and the clinopyroxene is Mg-augite, as in poikilitic harzburgites. Accessory minerals are primary orthopyroxene, with secondary phlogopite, amphibole and carbonate disseminated in the olivine-rich matrix (**Supplementary Fig. 1G, 1H**) or occurring in veins of plagioclase, ilmenite, rutile, sulphides and carbonate cross-cutting xenoliths.

The protogranular harzburgites have olivine Mg# (where $Mg\# = 100 \cdot Mg / (Mg + Fe)$) > 91, clinopyroxene Mg# > 92, and spinel Cr# ($\approx 40-60$; where $Cr\# = 100 \cdot Cr / (Cr + Al)$), far more refractory than primitive mantle mineral compositions (**Fig. 3F**). Poikilitic peridotites commonly display olivine, clinopyroxene, orthopyroxene and spinel with lower Mg# and higher Fe, Ti, Al, Na in Mg-augite and Opx. Most clinopyroxene grains in poikilitic peridotites have major element abundances lower than the primitive mantle estimate, especially in Ca, Ti, Al but they have higher Si, Na and Mg# associated with higher Mg# in olivine and Cr# in spinel (**Fig. 3**). Olivine and clinopyroxene in the dunites almost always have lower Mg# ($\sim 90-85$ and $\sim 92-87$, respectively) than protogranular harzburgites, and are in the range of compositions of poikilitic harzburgites or even lower (**Fig. 3**). Clinopyroxene grains in these rocks have higher contents of Ca, Ti but lower Al compared to primitive mantle. Hydrous mineral-bearing dunites have olivine and clinopyroxene with almost similar Mg# as anhydrous dunites, but their clinopyroxene has higher Na for similar ranges in Al, Ti, Ca. Spinel in dunites display a different range of composition based on the presence or absence of hydrous minerals; in anhydrous dunites spinel has lower Cr# ($\approx 17-49$) than protogranular harzburgites but similar Mg# ($\approx 82-52$), whereas hydrous dunites contain spinel with lower Mg# ($\approx 62-37$) and higher Cr# ($\approx 31-69$) than anhydrous dunites.

Two-pyroxene geothermometry (Brey and Köhler 1991) from co-existing pyroxenes indicates the protogranular harzburgites equilibrated at between 845-1005°C (assuming a pressure of 1.5 GPa; Grégoire et al., 2000a). These temperatures are lower than those of the Lac Michèle harzburgites (1050-1200°C Wasilewski et al., 2017) and the poikilitic peridotites (1015-1135°C). The range of calculated equilibrium temperatures in the dunites is difficult to determine due to the general absence

of orthopyroxene but, where this mineral occurs with clinopyroxene, the temperature estimates are 940-1090°C.

Bascou et al. (2008) interpreted the lattice-preferred orientations (LPO) of olivine and orthopyroxene in harzburgites to reflect a deformation regime in axial compression or transpression. They also showed that the fabric strength of olivine progressively decreases from protogranular harzburgite to poikilitic peridotite to dunite, in response to prolonged melt-rock reactions. The petrophysical parameters (Vp, density) of one type I poikilitic harzburgite xenolith (harzburgite GM92-453), representative of the average major element compositions of peridotite mantle xenoliths from Kerguelen, were determined by Grégoire et al. (2001). The measured and calculated Vp at 0.9 GPa were 8.45 km/s and 8.29 km/s, respectively. The seismic properties calculated from the LPO of minerals indicate that metasomatism at high melt/rock ratio lowers the P-wave velocities, and that the most significant difference between harzburgites and dunites corresponds to the distribution of S wave anisotropy. Thus, metasomatism by the Kerguelen Plume may have induced seismic heterogeneities in the lithospheric mantle (Bascou et al., 2008). The measured and calculated densities (3.30 and 3.34 g/cm³, respectively) indicate that the lithospheric mantle beneath Kerguelen Archipelago, assuming it is dominated by harzburgite as indicated by the xenoliths, should therefore be relatively buoyant and corroborates geophysical studies that interpret the occurrence of relatively low-density material down to a depth of about 80 km (e.g. Charvis et al., 1995).

2.3 Kerguelen xenolith major and trace element geochemistries

As the main and most common host of trace elements, clinopyroxene has been analysed by LA-ICP-MS in most Kerguelen peridotites types. Clinopyroxene grains in protogranular harzburgites have heterogeneous rare earth element (REE) element patterns that range from spoon-shaped patterns with heavy REE (HREE) and middle REE (MREE) contents of ≈ 0.2 times Chondrite to light REE-enriched (LREE) > 100 times CI-Chondrite (**Fig. 4A**). Clinopyroxenes in some Lac Michèle protogranular harzburgites have even lower MREE and LREE down to 0.05 X CI-Chondrite (**Fig. 4B**). Most protogranular clinopyroxene grains display spoon-shape REE patterns (**Fig. 4A and B**), and are accompanied by pronounced enrichments in Rb, Th, U, Pb \pm Sr but depletions in Ba, Nb, Zr and Ti (not shown). In contrast, clinopyroxene grains in poikilitic peridotites display similar REE patterns that are enriched in LREE (**Fig. 4C**) as well as in other very incompatible elements (Th, U, HFSE; see

Grégoire et al., 2000a). These clinopyroxenes are also more enriched in the most incompatible elements (LREE, **Fig. 4C**; HFSE or LILE; see Grégoire et al., 2000a) compared to the protogranular harzburgites. Clinopyroxene trace element contents in anhydrous dunites are similar to those in hydrous dunites (**Fig. 4D**) and, as a whole, the LREE and MREE-enriched clinopyroxenes in dunites resemble those in poikilitic peridotites. Some clinopyroxenes in anhydrous dunites have flat REE patterns or show depletions in the most incompatible elements compared to MREE and HREE (LREE, Fig 5D; also LILE, HFSE, see Grégoire et al., 2000 for details). Other samples show REE patterns with large enrichments in LREE associated with high Th, U and low Rb, Ba and HFSE. Clinopyroxene in the phlogopite-amphibole-bearing dunite MG91-143 shows the highest enrichment in the most incompatible elements (Th, U) and large depletions in HFSE (Nb, Ta, Zr, Hf, Ti). Clinopyroxene associated with carbonates in dunite GM92-140 displays lower enrichments of MREE over LREE and HREE, and high contents of Th, U associated with low HFSE contents (Moine et al., 2004).

Due to their large size, bulk rock major and trace elements have been measured in most Kerguelen peridotite types (**Supplementary Tables 2B and 2C**). The protogranular, poikilitic and Lac Michèle peridotites have refractory bulk rock major element compositions (**Fig. 5**), with low CaO (<1.35 wt %), Al₂O₃ (<1.5 wt %) and Na₂O (<0.25 wt %). The Mg# of the protogranular (91.5–92.0) and Lac Michèle (92.0–93.0) harzburgites are commonly higher than those of poikilitic peridotites (88.0 to 91.5). Protogranular harzburgites have low REE and display spoon-shaped-REE patterns characterized by (La/Sm)_N = 3.5–15 and (Sm/Yb)_N as low as 0.2 (subscript N; measured values normalized to primitive mantle values of McDonough&Sun, 1995). Some of those harzburgites, which display modal metasomatism by carbonate-rich melts, also show LREE-enriched patterns [La/Sm]_N varying between 2 and 6 similar to the poikilitic harzburgites (**Fig. 4B**; Delpech et al., 2004). Poikilitic harzburgites have enriched LREE and MREE contents compared to HREE and their total REE contents are higher than protogranular harzburgites (**Fig. 4C**; see Grégoire et al., 2000a) with (La/Sm)_N = 1.7–10.9 and (Sm/Yb)_N = 2.5–4.3.

Dunite samples tend to exhibit low SiO₂ for a similar range in MgO compared to harzburgites (**Fig. 5A**) and low CaO (0.18–1.6 wt %), Na₂O (< 0.27 wt %), Al₂O₃ (0.15–1.91 wt %; **Fig. 5B**), TiO₂ (0.03–0.09 wt %) contents, but their Mg# (85–89, average of 88) is lower than most of the

harzburgites (**Fig. 5C**). Dunite CaO and Al₂O₃ contents are sometimes higher than those in harzburgites (**Fig. 5C**), which reflects the relatively high modal content of clinopyroxene and spinel (Grégoire, 1994). The dunites are characterized by variable REE shapes compared to harzburgites, with a combination of almost flat REE patterns, LREE-enriched patterns and upward convex REE patterns (not shown, see Grégoire et al., 2000a).

2.4 Kerguelen peridotite Isotopic compositions

Bulk rock Os isotopic compositions from restricted suite of harzburgite, lherzolite and dunite xenoliths ($^{187}\text{Os}/^{188}\text{Os} = 0.1189\text{--}0.1383$; $n=19$; Hassler, 1998; Hassler & Shimizu, 2000) extend from unradiogenic values (0.1189) with rhenium-depletion model ages (T_{RD}) as old as 1.36 Ga to compositions more radiogenic than PUM (0.1296; Meisel et al. 2001). The radiogenic values are similar to Os isotope compositions of Kerguelen basalts, and may therefore represent the signature of mantle accreted by the Kerguelen plume (Weis et al., 2000).

Sr-Nd \pm Pb isotopes analysed for bulk rock ($n=13$) and clinopyroxene separates ($n=10$) from harzburgites, dunites, two lherzolites and one clinopyroxenite show very heterogeneous compositions (**Fig. 6**; Mattioli et al., 1996, 1999; Hassler, 1999). Most of the peridotite xenoliths have isotopic compositions in the range of $^{87}\text{Sr}/^{86}\text{Sr} = 0.7050\text{--}0.7065$, $^{143}\text{Nd}/^{144}\text{Nd} = 0.5123\text{--}0.5127$ and $^{206}\text{Pb}/^{204}\text{Pb} = 18.0\text{--}18.5$; $^{207}\text{Pb}/^{204}\text{Pb} = 15.50\text{--}15.65$; $^{208}\text{Pb}/^{204}\text{Pb} = 38.5\text{--}39.2$. These values are distinct from basalts of the Southeast Indian Ridge and rather similar to those of Kerguelen Archipelago lavas or even more enriched compositions (Mattioli et al., 1996, 1999; Hassler, 1998). Peridotites showing fingerprints of metasomatism by carbonatitic melts seem to extend to more enriched Sr-Nd isotopic compositions than those metasomatized by alkaline basaltic silicate melts. Their Sr-Nd isotope signature is similar to young (< 10 Ma) Kerguelen volcanic rocks and is comparable to the least evolved Heard Island lavas (Barling et al., 1994) (**Fig. 6**). A few samples show extreme Sr-Nd isotopic compositions; the most “depleted” end of the spectrum is represented by one little-metasomatized harzburgite that has clinopyroxene with unradiogenic $^{87}\text{Sr}/^{86}\text{Sr}$ of 0.70329 (OB93-78; Hassler, 1999), which falls in the field of Indian MORB (**Fig. 6**). Two samples (one anhydrous dunite and one Phl-bearing clinopyroxenite; Mattioli et al., 1999; Hassler, 1999) show very radiogenic $^{87}\text{Sr}/^{86}\text{Sr}$ (0.70730 and 0.70869) and unradiogenic $^{143}\text{Nd}/^{144}\text{Nd}$ (0.51215 and 0.51199) and are isotopically very different from the Kerguelen basalts, as they extend towards Sr-Nd isotopes found in continental crust material

recovered at Elan Bank (**Fig. 6**; Frey et al., 2002; Ingle et al., 2002) or volcanics highly contaminated by continental crust material (Site 738, **Fig. 6**). Such Sr-Nd isotope signatures indicate that some xenoliths interacted with or were formed from very evolved metasomatic melts or fluids percolating in the lithospheric mantle ; either of plume origin or by interaction with recycled continental lithosphere (Mattielli et al., 1999). It has been argued in the literature that the typical EM1 isotope signature of the Kerguelen basalts reflect that of melts produced by the Kerguelen plume (Weis et al., 1993).

2.5 Synthesis of the Kerguelen peridotitic mantle lithosphere

The type-I Kerguelen xenoliths show the peridotitic lithospheric mantle beneath this archipelago to largely be a refractory domain. The very low clinopyroxene vol.%, olivine Mg# up to 92 and Cr-rich spinel ($Cr\# > 38$), low HREE contents and MREE in some clinopyroxenes, and high bulk rock MgO and low CaO, Al_2O_3 , Na_2O , Fe_2O_3 , S and platinum group elements indicate that the underlying mantle experienced partial melting in excess of 15 to 25%, close to or beyond the exhaustion of clinopyroxene (**Fig. 4**; Grégoire et al. 1997 and 2000, Lorand et al., 2004). Clinopyroxenes with moderate HREE contents in **Fig. 4A** and **4B** are consistent with melting in the spinel stability field at low P (< 2 GPa), however clinopyroxenes in **Fig. 4A** and **4B** with low (HREE/HREE) ratios (eg. Dy/Yb) and the lowest HREE (Er, Yb, Lu) contents, lower than those predicted by 24% melting at low P, may be explained by polybaric melting initiated at higher P (> 2 GPa). Based on bulk-rock trace element modelling using melting equations of Walter (1998), Hassler (1999) showed that the REE abundances of a residual clinopyroxene after polybaric melting starting at 3 GPa and terminating at low P in the spinel facies is similar to those of clinopyroxenes in protogranular samples with the lowest HREE contents (**Fig. 4A**). The most depleted clinopyroxenes in the Lac Michèle harzburgites (**Fig. 4B**), characterized by low (HREE/HREE; eg. Dy/Yb) ratios and low HREE contents, can also be explained in a similar way. This idea is supported by Wasilewski et al. (2017), who also interpreted the more refractory bulk compositions of the Lac Michèle harzburgites to record evidence of polybaric decompression fractional melting between 5 and 3 GPa, initiated at high pressure in the garnet stability field (**Fig. 5B, 5D**). The Kerguelen peridotites have petrographic, mineralogical and geochemical compositions are different from abyssal peridotites (**Fig. 5B**) or the local Indian oceanic lithosphere (**Fig. 3, 6**) but are comparable to oceanic island peridotites worldwide (**Fig. 5**; Simon et al., 2008). Those authors suggested that depleted and therefore buoyant peridotite domains (OI1-u

peridotites from Simon et al. (2008)) such as Kerguelen peridotites, were accreted to the oceanic lithosphere from the convecting mantle by the ascending plume. Simon et al. (2008) proposed that reworking of older oceanic or subduction-related mantle domains from the convecting mantle is also consistent with the occurrence of some rhenium-depletion model ages far older than the Kerguelen lithosphere. Conversely, Hassler & Shimizu (1998) interpreted these Proterozoic rhenium-depletion model ages as an evidence for the occurrence of fragments of old subcontinental mantle domains that were incorporated into the Indian oceanic lithosphere during Gondwana breakup. Based on their modal and bulk major element compositions that resemble cratonic peridotites (**Fig. 5A, B, D**), the Lac Michèle harzburgites were also considered by Wasilewski et al. (2017) in the same manner as Hassler & Shimizu (1998). However, the low Mg# in olivine (91-92) for a given Cr# in spinel (**Fig. 3F**; or modal olivine contents in bulk rocks-not shown) compared to cratonic peridotites (**Fig. 5**) and lack of Os isotopes data on these peridotites do not yet allow a definite interpretation on their origin, especially considering that the existing Os isotopes data on Kerguelen are within the overall range of data found in modern oceanic lithospheric mantle (Pearson et al. 2007; Chatterjee and Lassiter, 2016; Day et al. 2017) or in oceanic plume settings (Simon et al., 2008).

The mineralogy and geochemistry of Kerguelen type-I peridotite xenoliths also require that the refractory mantle has experienced extensive post-depletion melt-rock reaction between ascending magmas (e.g. Grégoire et al. 1997; 2000a,b, Mattielli et al., 1996; 1999; Delpech et al., 2004; 2012; Moine et al., 2001; 2004; Schiano et al., 1994; Lorand et al., 2004). For instance, the occurrence of metasomatic minerals in peridotites (amphibole, phlogopite, carbonate, apatite), the enrichment in LREE (and very incompatible trace elements), Na, Fe, Ti, Al in some clinopyroxenes are indicative of melt-rock reactions (**Fig. 3, 4**). The metasomatic fingerprints of Kerguelen protogranular harzburgites and poikilitic peridotites may result from circulation within the upper mantle of primary CO₂-bearing alkaline to high-alkaline silicate melts closely linked to the magmatic activity of the Kerguelen plume (Grégoire et al., 2000; Lorand et al., 2004; Delpech et al., 2012). The Sr-Nd-Pb isotopic characteristics of the mantle xenolith suite, similar to Kerguelen basaltic lavas (Mattielli et al., 1996; 1999, Hassler, 1999), indicate metasomatism by ascending plume-derived magmas on their way to the surface. Mantle wall-rock interaction with such ascending magmas at low to high melt/rock ratio resulted in the different xenolith types (Grégoire et al., 1997; 2000a). Cryptic metasomatism at low melt/rock ratios affected the refractory protogranular harzburgites and caused slight enrichment in the

most incompatible trace elements (e.g. **Fig. 4A, 4B**). Poikilitic peridotites, however, experienced metasomatism at a higher melt/rock ratio, causing olivine and Mg-augite precipitation at the expense of orthopyroxene. As a result of interaction with Fe-bearing alkaline silicate melts at high melt/rock ratio, minerals in poikilitic rocks have lower Mg# and their clinopyroxene higher contents of Al, Ti, Na and incompatible trace elements but commonly less Ca than those of protogranular harzburgites (**Fig. 3**). Additionally, some of these Mg-augite grains also have trace element contents in near-equilibrium with alkaline basaltic silicate magmas erupted at the surface, supporting a genetic link with such magmas.

The dunites are considered to represent end-products of reaction of harzburgite with fluids at high melt/rock ratio, causing total resorption of orthopyroxene and crystallization of olivine and secondary clinopyroxene (Grégoire et al., 1997; 2000a). The common occurrence of composite xenoliths where dunite is the wall-rock of small dykes of websterite, clinopyroxenite or hornblende attest to a genetic relationship between dunite formation and magma percolation. Dunites with or without veins have a similar range of compositions suggesting that all the Kerguelen dunites are end products of such reaction processes between a former harzburgitic protolith and basaltic silicate melt (Grégoire et al., 1997; 2000a). This evolution is indicated in Figure 3 by the progressive decrease of Mg# of minerals in anhydrous or hydrous dunites, associated with increasing modal olivine contents, and the enrichment in Al, Ti, Na in clinopyroxene (Grégoire et al., 1997; 2000a). Some clinopyroxenes in dunites have trace element contents (**Fig. 4**) which are in near-equilibrium with various type of magmas erupted at the surface; ranging from early tholeiitic-transitional magmas to younger alkaline or highly alkaline magmas (see Grégoire et al. 1997, 2000a; Moine, 2000; Hassler, 1999). This is supported by their very variable Sr-Nd isotopes (**Fig. 6**) which cover a large spectrum of the Kerguelen volcanics but also extend well outside the field for Kerguelen volcanics (30-0 Ma) towards very evolved Sr-Nd isotopic compositions for a few samples. Mattielli et al. (1999) argued that the evolved Sr-Nd (and low Pb) signature of dunite MG91-114 (**Fig. 6**) reflects mixing of plume melts with melts derived from recycled continental crustal material. The radiogenic Os isotopes compositions of wherlitic dunites (Hassler & Shimizu, 1998) are however similar to Os isotope of Kerguelen basalts. Hence, dunite bodies probably formed in the lithospheric mantle at different times in the history of the Kerguelen Islands as the geodynamic setting changed; their mineralogical and geochemical compositions show they essentially equilibrated with metasomatic melts/fluids derived from the

Kerguelen plume. The occurrence of hydrous minerals in dunites such as phlogopite and/or amphibole, as in some harzburgites, has been attributed to younger metasomatic events by small volumes of fluid-enriched-alkaline or highly alkaline magmas, such as those forming the young lamprophyres at the surface (Grégoire et al. 2000a; Moine et al, 2001b; Hassler, 1999). For instance, Moine et al. (2001b) showed that disseminated amphibole in dunitic wall-rocks of hornblendite veins have geochemical compositions genetically related to those in the hornblendite veins, the later having trace element composition similar to young ultramafic silica-undersaturated highly alkaline lavas from Kerguelen (Moine et al., 2001). The occurrence of interstitial Mg-bearing calcites in pockets disseminated in some dunites (GM92-140; **Fig. 4D**; **Supplementary Fig. 1G**; Moine et al., 2004) that are very enriched in the most incompatible trace elements, may reflect metasomatism by small melt fractions of carbonate-rich melts shortly before eruption of the xenoliths. In some metasomatized harzburgites, carbonate-rich, alkaline silicate-rich and CO₂ inclusions have been found physically connected forming trails along fracture planes, and this led Schiano et al. (1994) to suggest a genetic relationship between both types of metasomatic fluids. It may be postulated that the original fluid-bearing alkaline basaltic silicate melts formed by the Kerguelen plume that metasomatized the lithospheric mantle and formed poikilitic peridotites and dunites, evolved into small volumes of volatile-rich melts following extensive percolation-reaction-crystallization processes. In this view, carbonate-rich melts/fluids may be formed by continuous reaction of an originally volatile-bearing alkaline silicate melt and do not require melting of a specific mantle source.

The Kerguelen lithospheric mantle record a complex and multi-stage evolution. The peridotite xenoliths indicate that they were formed by a high degree of melting, possibly in the garnet stability field. Their mineralogical and geochemical compositions were later sometimes strongly modified by the circulation of metasomatic fluids originating from the Kerguelen plume.

3.1 SUBANTARCTIC MANTLE UNDER THE SOUTHERN OCEAN

There are three known occurrences of Subantarctic mantle material exhumed in the Southern Ocean: the Auckland Islands, Macquarie Island and Campbell Island (**Fig. 1**, **Table 1**, **Supplementary Table 3**). The Auckland Islands comprise two intersecting glaciated early to middle Miocene intraplate shield volcanoes, the Ross and Carnley volcanoes, located just east of the steep descent to the adjacent oceanic lithosphere-floored Eocene-Oligocene Emerald Basin (**Fig. 7**) (Scott and Turnbull 2019). The

island group is dominated by Early Miocene basaltic to rhyolitic lava flows, tuffs, dykes and basaltic and gabbroic plugs that erupted through the Zealandia continental crust (Wright 1967, 1968, 1969; Gamble et al. 2018; Scott and Turnbull 2019). Peridotite xenoliths have been collected and analysed from one location, Mt Eden, in the northern Ross Volcano (Scott et al. 2014b, 2019). Macquarie Island, on the other hand, is a slice of exhumed Miocene oceanic lithosphere located on the southwest of the Emerald Basin on the transform boundary separating the Australian and Pacific plates (**Fig. 7**). It represents young oceanic lithosphere that formed after the 84 Ma Cretaceous separation of Zealandia and Australia. It is dominated by gabbro and mafic dikes, with serpentinised peridotite occurring in the northern portion (Goscombe & Everard, 1998; Wertz, 2003; Dijkstra et al., 2009). No peridotite has been found on the Campbell Island volcano, although coarse detrital xenocrystic zircon grains have been panned from clays. Trace elements, oxygen isotopes and U-Pb and Hf isotopes indicate these grains were derived from metasomatised mantle (van der Meer et al. 2019).

3.2.1 Auckland Islands peridotites

The inspected Auckland Islands mantle xenoliths are very fresh lherzolite and harzburgite, with the spinel textures, mineral chemistries and calculated equilibration indicating there to be two prominent types herein referred to as **Type 1** and **Type 2**. The **Type 1** xenoliths have coarse textures (**Supplementary Fig. 2**) except for the porphyroclastic AMED-3. Average olivine compositions for Type 1 peridotites range from Mg# = 89.8 to 90.7. Their spinel grains form blebs or holly-leaf shapes (e.g., **Supplementary Fig. 2A**) and have Cr# = 10.4-16.1 (**Supplementary Table 3A**). In contrast to the Type 1 rocks, **Type 2** xenoliths have higher olivine Mg# with average compositions ranging from 90.7-91.3. Spinel grains also have higher Cr# (22.9-31.5) than the Type 1 peridotites and form symplectitic textures with pyroxene (**Supplementary Fig. 2B**). There is one exception that does not fit either the Type 1 or Type 2 classification: AMED-11, which has olivine Mg# of ~87.5. Orthopyroxene in all Auckland Island peridotites is zoned, with MgO decreasing and Al₂O₃ and CaO increasing towards the rims. Clinopyroxene CaO and Al₂O₃ decrease towards the rims whereas MgO and FeO tend to increase. The rim-core trends in the Type 2 xenoliths are not quite as clear in clinopyroxene but nonetheless there is an increase in CaO (AMED-4, 5) and Al₂O₃ (AMED-5,6). Water contents measured by Fourier transform infrared spectrometry for olivine (calculated to be 6 to 26 ppm),

clinopyroxene (60 to 264 ppm) and orthopyroxene (28 to 125 ppm) indicate the peridotites to be fairly dry (Li et al. 2018).

Geothermometric calculations reveal a complex cooling history and a stratification to the Auckland Islands mantle. Using the Taylor (1998) Fe-Mg exchange geothermometer (with temperatures calculated assuming 15 kbar, although varying the P by 5 kbar makes $< 30^{\circ}\text{C}$ difference) on the cores of adjacent orthopyroxene and clinopyroxene grains shows the Type 1 peridotites to yield temperatures $< 950^{\circ}\text{C}$ whereas the Type 2 peridotites have temperatures ($> 1050^{\circ}\text{C}$) (**Supplementary Table 3B**). AMED-10, which has Type 1 chemistry, yields an intermediate temperature (1023°C), and the chemically anomalous AMED-11 has a high temperature (1134°C). If the Auckland Island xenoliths were extracted along a single geotherm, then 1) the Type 1 peridotites are from shallower than the Type 2 peridotites and 2) the large ($\sim 300^{\circ}\text{C}$) spread temperatures for rocks that all belong to the spinel facies requires a heat flow of $\sim 70 \text{ mW m}^{-2}$ (**Fig. 8**). This is similar to the Late Oligocene-Miocene heat flow calculated for elsewhere in Zealandia (Scott et al. 2014a, b). However, since clinopyroxene incorporates more CaO and less MgO with higher temperatures (Bertrand and Mercier, 1985), the orthopyroxene Ca-rimward increase and clinopyroxene Ca-rimward decrease in adjacent grains in the Auckland Island suite indicates the mantle column also experienced a small temperature increase. Orthopyroxene analyses that fall within the compositional bounds of the Witt-Eickschen & Seck (1991) Cr-Al-orthopyroxene geothermometer (AMED-6 and AMED-7; the other samples tend to have too much Al in the M1 site) indicate that the pyroxene rims record a temperature rise of up to 80°C . Although the changes could be due to heating of the xenoliths in the host magma, this would not have promoted such large diffusion profiles since element exchange of Ca in clinopyroxene is slow (e.g., a 0.15 mm wide profile at 1000°C would take $\sim > 1000$ years; Zhang et al., 2010; Dalton et al., 2017).

Trace elements from the cores of clinopyroxene grains also support the interpretation of a stratified mantle beneath the Auckland Islands. The Type 1 clinopyroxenes form a tight compositional cluster with HREE concentrations around $10 \times$ chondrite but low concentrations of LREE (**Fig. 9A**). When compared with theoretical compositions calculated for different degrees of melting (Scott et al. 2016), the Type 1 data deviate little from the area of low degree melting. In comparison, the clinopyroxenes from hotter Type 2 xenoliths have distinctly lower HREE contents, with the middle and

LREE showing dramatic departure from the melting curves consistent with enrichment of depleted residues by a LREE-bearing fluid (**Fig. 9B**). Elsewhere in Zealandia, this type of enrichment, coupled with Ti/Eu ratios has been interpreted to result from Mesozoic carbonatitic or CO₂-rich silicate fluids (Scott et al. 2014a, b; McCoy-West et al. 2015, 2016; Scott et al. 2016; Dalton et al., 2017).

In an adiabatic melting column, the most depleted residues should be those that undergo the most decompression melting and are thus the shallowest in the end process of melting. This logic makes the configuration of a less-depleted mantle domain (Type 1) residing above a highly-depleted mantle domain (Type 2) unusual and would require some form of tectonic juxtaposition. An added complication is that the pyroxenes from both appear to record a slight temperature increase that likely predates the xenolith entrainment. This thermal increase may be due to the rifting and formation of oceanic lithosphere in the adjacent Emerald Basin (**Fig. 7**), which occurred in the Eocene-Oligocene before the intraplate Auckland Islands formed.

3.2.2 Macquarie Island peridotite

In contrast to the fresh Auckland Island peridotites, the freshest Macquarie Island peridotites at best retain up to 60% primary minerals and most are thoroughly serpentinised (Wertz, 2003; Dijkstra et al. 2009) (**Supplementary Fig. 2C**). Olivine and orthopyroxene are commonly partially to totally altered to serpentine or bastite, respectively, with abundant magnetite, and minor talc, amphibole and carbonate occurring as secondary phases. Although Dijkstra et al. (2009) show images with relict olivine grains amongst serpentine, they provided no chemical analyses and our own samples and those of Wertz (2003) have no olivine preserved. However, the Cr-rich nature of spinel (Cr# = 39 to 49; Wertz, 2003; Dijkstra et al. 2009) indicates that these underwent moderate levels of melt extraction, which is consistent the very low clinopyroxene modal percentage (< 2 %); the peridotites were therefore likely harzburgitic prior to alteration. This interpretation is supported by the HREE concentrations of clinopyroxene grains (Dijkstra et al., 2010), which when compared to theoretical depleted clinopyroxene compositions indicate that the peridotite experienced 20 to > 25% partial melt depletion (**Fig 9C**). However, the clinopyroxene analyses also reveal that the Macquarie Island mantle has been subsequently enriched in LREE, with compositions varying widely within single samples (Wertz, 2003; Dijkstra et al. 2009) (**Fig 9C**). Equilibrium temperatures have not been calculated for the Macquarie Island peridotites as it is not clear if the clinopyroxene and orthopyroxene grains are in

equilibrium. Nonetheless, the rimward decrease in Al_2O_3 in orthopyroxene (Dijkstra et al. 2010) and diffusion rates of Al in opx may mean that the mantle experienced slow cooling.

3.3 Auckland Island and Macquarie Island isotopes

3.3.2 Os isotopes

Osmium isotopes are reported for 15 Auckland Island peridotites, for which 7 were reported by Scott et al. (2019) and 8 are new (all are summarised in the **Supplementary Table 3B**). The Auckland Island Type 1 peridotites have $^{187}\text{Os}/^{188}\text{Os}$ of 0.1222 to 0.1299 with Re-depletion modal ages (TRD) ranging up to 0.87 Ga but clustering at ~ 0.4 Ga (**Fig. 10A**). The Type 2 peridotites extend to slightly less radiogenic Os values than the Type 1 xenoliths, with $^{187}\text{Os}/^{188}\text{Os} = 0.1183$ to 0.1248 and Re-depletion Os model ages of 0.68 to 1.58 Ga. These results overlap with the Os isotope and model ages of other suites of peridotite erupted through the Zealandia continental lithosphere (**Fig. 10A**) (McCoy-West et al., 2013; Liu et al., 2015; Scott et al., 2019), although both Auckland Island suites are at the more fertile Al_2O_3 end of the Zealandia spectrum (**Fig. 10B**). The Auckland Island $^{187}\text{Os}/^{188}\text{Os}$ data are very similar to the oceanic lithospheric mantle associated with Kerguelen, the Dun Mountain Ophiolite Belt and modern abyssal peridotite (**Fig. 10A**). Platinum group elements (PGE) show that many of the Auckland Island Type 1 xenoliths and one of the Type 2 xenoliths have higher Pd/Ir than PUM (**Supplementary Table 3B; Fig. 10C**), which indicate that the PGE in these samples have been disturbed via metasomatism. These Type 1 data are, however, similar to the ultramafic portion of the Dun Mountain Ophiolite Belt (**Fig. 10A, B**) (Scott et al. 2019), which is a Permian oceanic lithosphere accreted to Zealandia.

Despite Macquarie Island having a Miocene lithosphere stabilisation age, the peridotites have $^{187}\text{Os}/^{188}\text{Os} = 0.1194$ to 0.1227 and ancient Re-depletion Os model ages of 0.73 to 1.23 Ga (**Fig. 10A**) (Dijkstra et al. 2010; **Supplementary Table 3B**). These data are similar to Kerguelen, Auckland Islands Type 2 and abyssal peridotite data. An implication of the Auckland Island, Kerguelen and Macquarie Island Os isotope data is therefore that Subantarctic mantle probably contains significant amounts of peridotite that is 100s of millions to billions of years older than the overlying crust. Since peridotite on Macquarie Island represents decompressed asthenosphere accreted to form lithosphere, these anomalies must also be present in the convecting mantle in the Subantarctic.

Sr-Nd-Pb and Hf isotopes on the Auckland Islands or Macquarie Island are restricted to reconnaissance studies. A small dataset of 4 clinopyroxene $^{87}\text{Sr}/^{86}\text{Sr}$, $^{143}\text{Nd}/^{144}\text{Nd}$ and $^{206}\text{Pb}/^{204}\text{Pb}$, $^{207}\text{Pb}/^{204}\text{Pb}$ and $^{208}\text{Pb}/^{204}\text{Pb}$, and two $^{176}\text{Hf}/^{177}\text{Hf}$ analyses was described from the Auckland Islands by Scott et al. (2014b). The lowest $^{87}\text{Sr}/^{86}\text{Sr}$ (0.70231) and highest $^{143}\text{Nd}/^{144}\text{Nd}$ (0.51332) occurs in the Type 1 AMED-7 (**Supplementary Table 3B**), whereas the three analysed Type 2 xenoliths have slightly more radiogenic $^{87}\text{Sr}/^{86}\text{Sr}$ (0.70282 to 0.70293) and variable $^{143}\text{Nd}/^{144}\text{Nd}$ (0.51294 to 0.51325). Due to the low concentrations, Pb isotopes have only been obtained from clinopyroxene separates in the Type 2 rocks. These yielded $^{206}\text{Pb}/^{204}\text{Pb} = 19.5$ to 20.2 , $^{207}\text{Pb}/^{204}\text{Pb} = 15.6$ to 15.7 , and $^{208}\text{Pb}/^{204}\text{Pb} = 39.1$ to 40.0 . ϵHf data show Type 1 AMED-7 to have $\epsilon\text{Hf}_{(16\text{ Ma})} = +22$ and Type 2 AMED-5 to have extremely radiogenic $\epsilon\text{Hf} = +85$, with this latter value being decoupled from the Nd and Sr isotopic record but within the range of abyssal peridotites from modern oceanic lithosphere (e.g. Stracke et al., 2011). The clinopyroxene Sr and Nd isotopes for clinopyroxene from 6 Macquarie Island peridotites fall between $^{87}\text{Sr}/^{86}\text{Sr}$ of 0.70256 to 0.70322 and $^{143}\text{Nd}/^{144}\text{Nd}$ of 0.51314 to 0.51305 (Dijkstra et al. 2010) and overlap with most of the Auckland Island data (**Supplementary Table 3B**). Furthermore, the data are also comparable to Sr-Nd-Pb-Hf data collected from peridotites erupted through continental lithosphere elsewhere in Zealandia (Scott et al., 2014a, b; McCoy-West et al., 2016; Dalton et al., 2017), which represent a combination of variable depletion ages overprinted by carbonatitic or related metasomatic melts.

4. SUBANTARCTIC LITHOSPHERIC MANTLE UNDER THE ATLANTIC OCEAN

Mantle peridotite xenoliths have not been found on Bouvet, South Georgia or the South Sandwich island groups in the Atlantic Ocean (**Fig. 1, 11**). However, samples of peridotite have been dredged from along the trench wall of South Sandwich Arc and at the intersection of the South Sandwich trench with the South American and Antarctic plates (Pearce et al. 2000), as well as along fracture zones along Subantarctic portions of the Southwest Indian Ridge and South America-Antarctic Ridge (e.g., Johnston et al., 1990; Jaroslow et al., 1996; Hellebrand et al., 2001; Snow and Dick, 1995; Brunelli et al. 2003; Warren et al., 2009) (**Fig. 11**). Since these occurrences have already been described in detail by other workers and we have no new information to complement existing data, the reader is guided to the aforementioned publications and Warren (2016) for detailed information, and only a brief summary is given here. The abyssal peridotites, in all cases are moderately to extensively serpentinised, with most estimated to have been harzburgite prior to hydration. Trace elements

collected from abyssal peridotite clinopyroxene grains indicate the rocks to have mostly undergone moderate depletion consistent with decompression melting (Hellebrand et al., 2001; Brunelli et al. 2003; Warren, 2016). Many of the clinopyroxenes also show some re-enrichment of light rare earth element abundances. The South Sandwich peridotites represent supra-subduction zone mantle and therefore a distinct geodynamic setting to the peridotites found at mid-ocean ridge fracture zones. These peridotites are, in general, more melt-depleted than the abyssal peridotites and are characterised by having spinels with very high Cr# at variable Ti contents, thought to indicate “up-grading” of the Cr# in spinel by melt-rock reaction with a variety of melts including those of boninitic composition. Like the abyssal peridotites, the supra-subduction zone peridotites appear to have been harzburgites prior to extensive serpentinisation, and the clinopyroxene trace elements show moderate depletion variable overprinted by LREE enrichment (Pearce et al. 2000).

Osmium, Sr, Nd and Pb isotopes from abyssal peridotite sulphide and pyroxene minerals indicate that portions of the mantle beneath the Subantarctic Southwest Indian Ridge were depleted billions of years before present-day (Warren et al. 2009; Warren and Shirey 2012; Day et al., 2017). Thus, like the Southern Ocean and Kerguelen occurrences discussed above, the modern convecting mantle beneath the southern Atlantic in the Subantarctic must contain ancient domains embedded within younger mantle, that stabilised as lithosphere during Mesozoic and more recent times.

5. CONCLUSIONS

Mantle peridotite occurs as xenoliths in intraplate basalts in the Subantarctic (between 46 and 60°S) Kerguelen and Heard islands in the Indian Ocean and on Auckland Island in Southern Ocean and represent samples of the lithospheric mantle from beneath these locations. Little is known about the Heard Island mantle lithosphere, but the Kerguelen and Auckland Island xenoliths were derived from lithosphere associated with the Kerguelen Plateau and Zealandia, respectively. The peridotite xenoliths are variably depleted, some to quite refractory levels especially from beneath Kerguelen and the South Sandwich Islands, and commonly contain complex metasomatic histories. The Auckland Islands mantle is distinctive as a result of it being chemically stratified, with apparently a fertile cooler and shallower layer underlain by a more depleted but metasomatised hotter domain – although further work elsewhere may find this to be a common occurrence. Osmium \pm Hf isotopes point to some of the Kerguelen and Auckland Island mantle fragments having undergone depletion 100s of millions to

billions of years before formation of the overlying and much younger crust. These ancient depletion events – as with those documented in abyssal peridotites from modern oceanic mantle – therefore cannot explain the timing of lithosphere formation as it currently is represented beneath these locations but more likely record evidence for more ancient events that produced residual mantle or minerals then incorporated into younger lithosphere.

Abyssal peridotite has been dredged from fracture zones along the Subantarctic portions of the South America-Antarctica and Southwest and Southeast Indian Ridges in the southern Atlantic and Indian Oceans. Although these abyssal peridotites are typically very serpentinised, most appear to have harzburgite protoliths. Serpentinised oceanic lithospheric peridotite has also been found exposed on Macquarie Island, which is an exhumed fracture zone that now forms part of the plate boundary separating the Pacific and Australian plates in the Southern Ocean. Like the Subantarctic mantle lithosphere associated with Kerguelen and Zealandia, Os isotopic analyses show the modern Subantarctic oceanic upper mantle must have embedded ancient peridotite fragments that have histories that long-predate the formation of the lithosphere.

ACKNOWLEDGEMENTS

Kerguelen archipelago research was funded by CNRS, St Etienne and Toulouse III Universities research programs and the Paul Emile Victor Institute field campaigns (IPEV, France) as well as the Australian Research Council and Macquarie University research programs (fundings to S.Y. O'Reilly, W.L. Griffin and G. Delpech). This is GEMOC publication number XXXX. Auckland Island research was funded by a Foundation for Science Research and Technology Fellowship (contract UOOX1004) to JMS, and a Canada Excellence Research Chair Funding to DGP and a 1000 Youth Talents Programme to J. Liu. S. Read (Otago) helped to generate the maps. Comments by A Stracke and A McCoy-West improved the paper.

REFERENCES

Aubert de la Rüe, E., 1932. Étude géologique et géographique de l'archipel de Kerguelen. *Revue de géographie physique et de la géologie dynamique*, 224 p.

- Bascou, J., Delpech, G., Vauchez, A., Moine, B.N., Cottin, J.Y., Barruol, G., 2008. An integrated study of microstructural, geochemical, and seismic properties of the lithospheric mantle above the Kerguelen plume (Indian Ocean). *Geochemistry, Geophysics, Geosystems*, 9, 4, 1-26.
- Bertrand, P., & Mercier, J. C. C. (1985). The mutual solubility of coexisting ortho-and clinopyroxene: toward an absolute geothermometer for the natural system? *Earth and Planetary Science Letters*, 76(1-2), 109-122.
- Brunelli, D., Cipriani, A., Ottolini, L., Peyve, A., & Bonatti, E. (2003). Mantle peridotites from the Bouvet triple junction region, south Atlantic. *Terra Nova*, 15(3), 194-203.
- Charvis p., Recq M., Operto S., Brefort D. 1995 - Deep structures of the northern Kerguelen plateau and hotspot related activity. *Geophysical Journal International*, 122, 899-924.
- Coffin, M. F., and O. Eldholm, 1993 - Scratching the surface: Estimating dimensions of large igneous provinces, *Geology*, 21, 515-518.
- Coffin, M.F., Pringle, M.S., Duncan, R.A., Gladchenko, T.P., Storey, M., Müller, R.D., Gahagan, L.A. 2002 - Kerguelen hotspot magma output since 130 Ma. *Journal of Petrology*, 43, 1121–1137.
- Dalton, H.B., Scott, J.M., Liu, J., Waight, T.E., Pearson, D.G., Brenna, M., Le Roux, P. and Palin, J.M., 2017. Diffusion-zoned pyroxenes in an isotopically heterogeneous mantle lithosphere beneath the Dunedin Volcanic Group, New Zealand, and their implications for intraplate alkaline magma sources. *Lithosphere*, 9(3), pp.463-475.
- Day, J. M., Walker, R. J., & Warren, J. M. (2017). 186Os–187Os and highly siderophile element abundance systematics of the mantle revealed by abyssal peridotites and Os-rich alloys. *Geochimica et Cosmochimica Acta*, 200, 232-254.
- Delpech, G., 2004. Trace element and isotopic fingerprints in ultramafic xenoliths from the Kerguelen Archipelago (South Indian Ocean). PhD thesis, Macquarie University, 331 p.

- Delpech, G., Grégoire, M., O'Reilly, S.Y., Cottin, J.Y., Moine, B., Michon, G., Giret, A. 2004 - Feldspar from carbonate-rich silicate metasomatism in the shallow oceanic mantle under Kerguelen Islands (South Indian Ocean). *Lithos* 75, 209–237.
- Delpech G., Lorand J.-P., Grégoire M., Cottin J.-Y., O'Reilly S. Y. 2012. - In-situ geochemistry of sulfides in highly metasomatized mantle xenoliths from Kerguelen, southern Indian Ocean. *Lithos*, 154, 296–314.
- Dijkstra, A. H., Sergeev, D. S., Spandler, C., Pettke, T., Meisel, T., & Cawood, P. A. (2010). Highly refractory peridotites on Macquarie Island and the case for anciently depleted domains in the Earth's mantle. *Journal of Petrology*, 51(1-2), 469-493.
- Dosso L., Vidal P., Cantagrel J.M., Lameyre J., Marot A., Zimine S. 1979 - "Kerguelen: Continental fragment or oceanic island?": Petrology and isotopic geochemistry evidence. *Earth and Planetary Science Letters*, 43, 46-60.
- Doucet S., Weis D., Scoates J.S., Nicolaysen K., Frey F.A., Giret A. 2002 - The depleted mantle component in Kerguelen archipelago basalts: petrogenesis of tholeiitic-transitional basalts from the Loranchet peninsula. *Journal of Petrology*, 43, 1341-1366.
- Doucet, S., Scoates, J.S., Weis, D., Giret, A., 2005 - Constraining the components of the Kerguelen mantle plume: a Hf-Pb-Sr-Nd isotopic study of picrites and high-MgO basalts from the Kerguelen Archipelago. *Geochemistry, Geophysics, Geosystems*, 6.
- Edwards A.B. (1938). Tertiary lavas from the Kerguelen Archipelago. B.A.N.Z. Antarctic Expedition, (D. Dawson) 1929-1931, Rep. A, 5, 2, 72-100.
- Frey F.A., Weis D., Yang H.J., Nicolaysen K., Leyrit H., Giret A. 2000 - Temporal geochemical trends in Kerguelen archipelago basalts: evidence for decreasing magma supply from the Kerguelen plume. *Chemical Geology*, 164, 61- 80.
- Gautier, I., Weis, D., Mennessier, J.-P., Vidal, P., Giret, A., Loubet, M., 1990 - Petrology and geochemistry of the Kerguelen Archipelago basalts (South Indian Ocean): evolution of the mantle sources from ridge to intraplate position. *Earth and Planetary Science Letters*, 100, 59–76.

- Gautier I., 1987 - les basaltes des îles Kerguelen (Terres Australes et Antarctiques Françaises).
Thèse de Doctorat, Univ. Paris VI, France, 383 p.
- Giret A., Grégoire M., Cottin J.Y., Michon G. 1997 - Kerguelen, a third type of oceanic island? In: "The Antarctic Region: Geological Evolution and Processes", C.A. Ricci ed., Terra Antarctica Publication, Siena, 735-741.
- Giret A. 1983 - Le plutonisme océanique intraplaque, exemple des îles Kerguelen. Thèse d'Etat, Bull. CNFRA, Paris, 54, 290p.
- Goscombe, B. D., & Everard, J. L. (1998). 1: 10000 Geological Map of Macquarie Island. *Mineral Resources, Tasmania*.
- Grégoire, M., 1994. Pétrologie des enclaves ultrabasiques et basiques des Iles Kerguelen. Les contraintes minéralogiques et thermobarométriques et leurs implications géodynamiques ? PhD thesis, Université Jean Monnet, 253 p.
- Grégoire M., Leyrit H., Cottin J.Y., Giret A. & Mattielli N. 1992 - Les phases précoces et profondes du magmatisme des îles Kerguelen révélées par les enclaves basiques et ultrabasiques. – Comptes Rendus de l'Académie des Sciences, Paris, 314, série II, 1203-1209.
- Grégoire, M., Mattielli, N., Nicollet, C., Cottin, J.Y., Leyrit, H., Weis, D., Shimizu, N., Giret, A. 1994 - Oceanic mafic granulite xenoliths from the Kerguelen archipelago. *Nature* 367, 360–363.
- Grégoire M., Cottin J.Y., Mattielli N., Nicollet C., Weis D. & Giret A. 1995) - The Kerguelen archipelago: a hypothetical continental mafic protolith. *Terra Antarctica*., 2 (1), 1- 6.
- Grégoire M. Cottin J.Y., Giret A., Mattielli N. & Weis D. 1996 - Mantle-melt interactions and magmatic underplating beneath the Kerguelen oceanic islands revealed by ultrabasic and basic xenoliths. *Petrology and Geochemistry of magmatic suites of rocks in the continental and oceanic crust: a volume dedicated to Professor Jean Michot. D Demaiffe (Ed) Université Libre de Bruxelles*, 371-384.

- Grégoire, M., Lorand, J.-P., Cottin, J.-Y., Giret, A., Mattielli, N., Weis, D. 1997 - Xenoliths evidence for a refractory oceanic mantle percolated by basaltic melts beneath the Kerguelen archipelago. *European Journal of Mineralogy*, 9, 1085–1100.
- Grégoire, M., Cottin, J.Y., Giret, A., Mattielli, N., Weis, D. 1998 - The meta-igneous granulite xenoliths from Kerguelen Archipelago: evidence of a continent nucleation in an oceanic setting. *Contributions to Mineralogy and Petrology*, 133, 259–283.
- Grégoire, M., Moine, B.N., O'Reilly, S.Y., Cottin, J.Y., Giret, A. 2000a - Trace element residence and partitioning in mantle xenoliths metasomatized by highly alkaline, silicate- and carbonate-rich melts (Kerguelen Islands, Indian Ocean). *Journal of Petrology*, 41, 477–509.
- Grégoire, M., Lorand, J.P., O'Reilly, S.Y., Cottin, J.-Y., 2000b - Armalcolite-bearing, Ti-rich metasomatic assemblages in harzburgitic xenoliths from the Kerguelen Islands: implications for the oceanic mantle budget of high-field strength elements. *Geochimica et Cosmochimica Acta*, 64, 673–694.
- Grégoire M., Jackson I., O'Reilly S. Y., Cottin J.-Y. 2001 - The lithospheric mantle beneath the Kerguelen Islands (Indian Ocean): petrological and petrophysical characteristics of mantle mafic rock types and correlation with seismic profiles. *Contributions to Mineralogy and Petrology*, 142, 244-259
- Harte, B. 1977 - Rock nomenclature with particular relation to deformation and recrystallization textures in olivine-bearing xenoliths. *Journal of Geology*, 85, 279-288.
- Hassler, D.R. 1999 - Plume lithosphere interaction: geochemical evidence from upper mantle and lower crustal xenoliths from the Kerguelen Islands. PhD thesis, MIT/WHOI, 368 p.
- Hassler D.R., Shimizu N. 1998 - Osmium isotopic evidence for ancient subcontinental lithospheric mantle beneath the Kerguelen Islands, Southern Indian Ocean. *Science*, 280, 418-421.
- Hasterok, D., & Chapman, D. S. (2011). Heat production and geotherms for the continental lithosphere. *Earth and Planetary Science Letters*, 307(1-2), 59-70.

- Kamenetsky, V. S., Everard, J. L., Crawford, A. J., Varne, R., Eggins, S. M., & Lanyon, R. (2000). Enriched end-member of primitive MORB melts: petrology and geochemistry of glasses from Macquarie Island (SW Pacific). *Journal of Petrology*, 41(3), 411-430.
- Klemme, S., & O'Neill, H. S. (2000). The near-solidus transition from garnet lherzolite to spinel lherzolite. *Contributions to Mineralogy and Petrology*, 138(3), 237-248.
- Jaroslow, G. E., Hirth, G., & Dick, H. J. B. (1996). Abyssal peridotite mylonites: implications for grain-size sensitive flow and strain localization in the oceanic lithosphere. *Tectonophysics*, 256(1-4), 17-37.
- Johnson, K. T., Dick, H. J., & Shimizu, N. (1990). Melting in the oceanic upper mantle: an ion microprobe study of diopsides in abyssal peridotites. *Journal of Geophysical Research: Solid Earth*, 95(B3), 2661-2678.
- Lameyre J., Marot A., Zimine S., Cantagrel J.M., Dosso L. & Vidal P., 1976 - Chronological evolution of the Kerguelen islands syenite-granite ring complexes. *Nature*, 263, 306-307.
- Le Roex, A. P., Chevallier, L., Verwoerd, W. J., & Barends, R. (2012). Petrology and geochemistry of Marion and Prince Edward Islands, Southern Ocean: Magma chamber processes and source region characteristics. *Journal of volcanology and geothermal research*, 223, 11-28.
- Leat, P. T., Smellie, J. L., Millar, I. L., & Larter, R. D. (2003). Magmatism in the South Sandwich arc. *Geological Society, London, Special Publications*, 219(1), 285-313.
- Leyrit H. 1992 - Kerguelen : cartographie et magmatologie des presqu'îles Jeanne d'Arc et Ronarc'h. Place des laves différenciées. Thèse Université Paris XI, 240 p.
- Li, P., Scott, J.M., Liu, J., Xia, Q.-K. (2018). Lateral H₂O variation in the Zealandia lithospheric mantle controls orogen width. *Earth & Planetary Science Letters*, 502, 200-209.
- Liu, J., Scott, J. M., Martin, C. E., & Pearson, D. G. (2015). The longevity of Archean mantle residues in the convecting upper mantle and their role in young continent formation. *Earth and Planetary Science Letters*, 424, 109-118.

- Liu, C. Z., Snow, J. E., Hellebrand, E., Brüggmann, G., Von Der Handt, A., Büchl, A., & Hofmann, A. W. (2008). Ancient, highly heterogeneous mantle beneath Gakkel ridge, Arctic Ocean. *Nature*, 452(7185), 311.
- Lorand, J.-P., Delpech, G., Grégoire, M., Moine, B., O'Reilly, S.Y., Cottin, J.Y. 2004 - Platinum-group elements and the multistage metasomatic history of Kerguelen lithospheric mantle (South Indian Ocean). *Chemical Geology*, 208, 195–215
- Meisel, T., Walker, R.J., Irving, A.J., Lorand, J.P., 2001. Osmium isotopic compositions of mantle xenoliths: a global perspective. *Geochimica et Cosmochimica Acta*, 65, 1311-1323.
- McCoy-West, A. J., Bennett, V. C., & Amelin, Y. (2016). Rapid Cenozoic ingrowth of isotopic signatures simulating “HIMU” in ancient lithospheric mantle: distinguishing source from process. *Geochimica et Cosmochimica Acta*, 187, 79-101.
- McCoy-West, A. J., Bennett, V. C., Puchtel, I. S., & Walker, R. J. (2013). Extreme persistence of cratonic lithosphere in the southwest Pacific: Paleoproterozoic Os isotopic signatures in Zealandia. *Geology*, 41(2), 231-234.
- McBirney, A. and Aoki, K.I. 1973 - Factors governing the stability of plagioclase at high-pressures as shown by spinel-gabbro xenoliths from the Kerguelen Archipelago. *American Mineralogist*, 58, 271-276.
- McDonough, W.F., Sun, S.-s, 1995. The composition of the Earth. *Chemical Geology*, 120, 223-253.
- Mattielli, N., Weis, D., Grégoire, M., Mennesier, J.P., Cottin, J.Y., Giret, A. 1996 - Kerguelen basic and ultrabasic xenoliths: evidence for long-lived Kerguelen hotspot activity. *Lithos*, 37, 261–280.
- Mattielli, N., Weis, D., Scoates, J.S., Shimizu, N., Mennessier, J.-P., Grégoire, M., Cottin, J.-Y., Giret, A. 1999 - Evolution of heterogeneous lithospheric mantle in a plume environment beneath the Kerguelen Archipelago. *Journal of Petrology*, 40, 1721–1744.
- Moine, B., Grégoire, M., O'Reilly, S.Y., Sheppard, S.M.F., Cottin, J.Y. 2001 - High field strength element fractionation in the upper mantle: evidence from amphibole-rich composite mantle xenoliths from the Kerguelen Islands (Indian Ocean). *Journal of Petrology*, 42, 2143–2167.

- Moine, B., Grégoire, M., O'Reilly, S.Y., Delpech, G., Sheppard, S.M.F., Lorand, J.-P., Renac, C., Giret, A., Cottin, J.Y. 2004 - Carbonatite melt in oceanic upper mantle beneath the Kerguelen Archipelago. *Lithos*, 75, 239–252.
- Moine, B. 2000 - Volatile-bearing Ultramafic to Mafic Xenoliths from the Kerguelen Archipelago (Southern Indian Ocean), Fluids Migration and Mantle Metasomatism within Oceanic Intraplate Setting. PhD thesis, Université Jean Monnet, St-Etienne, 281 p.
- Nixon, P. H. (1987). Mantle xenoliths. John Wiley & Sons Ltd.
- Nougier J. 1970 - Contribution à l'étude géologique et géomorphologique des îles Kerguelen. Thèse d'Etat, 2 volumes Bull. CNFRA, 27, t.1, 440 p., t.2, 256 p.
- Parkinson, I. J., Hawkesworth, C. J., & Cohen, A. S. (1998). Ancient mantle in a modern arc: Osmium isotopes in Izu-Bonin-Mariana forearc peridotites. *Science*, 281(5385), 2011-2013.
- Pearce, J. A., Barker, P. F., Edwards, S. J., Parkinson, I. J., & Leat, P. T. (2000). Geochemistry and tectonic significance of peridotites from the South Sandwich arc–basin system, South Atlantic. *Contributions to Mineralogy and Petrology*, 139(1), 36-53.
- Pearson, D. G., Parman, S. W., & Nowell, G. M. (2007). A link between large mantle melting events and continent growth seen in osmium isotopes. *Nature*, 449(7159), 202-205.
- Quilty, P. G., & Wheller, G. E. (2000). Heard Island and the McDonald Islands: a window into the Kerguelen Plateau. In *Papers and Proceedings of the Royal Society of Tasmania* (Vol. 133, No. 2, pp. 1-12).
- Royer J.Y., Coffin M.F. 1992 - Jurassic to eocene plate tectonics reconstruction in the Kerguelen plateau region. In: proc. ODP, Sci. Results, 120 (Wise S.W. Jr. et al., eds), pp. 917-928. College Station, Tx (Ocean Drilling Program).
- Schiano, P., Clocchiatti, R., Shimizu, N., Weis, D., Mattielli, N. 1994 - Cogenetic silica-rich and carbonate-rich melts trapped in mantle minerals in Kerguelen ultramafic xenoliths: Implications for metasomatized upper mantle. *Earth and Planetary Science Letters*, 123, 167-178.

- Scoates J.S., Weis D., Franssens M., Mattielli N., Annell H., Frey F.A., Nicolaysen K., Giret A. 2007 - The Val Gabbro Plutonic Suite: A sub volcanic Intrusion Emplaced at the End of Flood Basalt Volcanism on the Kerguelen Archipelago. *Journal of Petrology*, 49, 79–105.
- Scott, J. M., & Turnbull, I. M. (2019). Geology of New Zealand's Sub-Antarctic Islands. *New Zealand Journal of Geology and Geophysics*, 1-27.
- Scott, J. M., Liu, J., Pearson, D. G., Waight, T. E. (2016). Mantle depletion and metasomatism recorded in orthopyroxene in highly depleted peridotites. *Chemical Geology*, 441, 280-291.
- Scott, J.M., Turnbull, I.M., Auer, A., Palin, J.M. (2013). The Sub-Antarctic Antipodes Volcano: A < 0.5 Ma HIMU-like Surtseyan volcanic outpost on the edge of the Campbell Plateau, New Zealand. *New Zealand Journal of Geology & Geophysics*, 56(3), 134-153.
- Scott, J. M., Hodgkinson, A., Palin, J. M., Waight, T. E., van der Meer, Q. H. A., & Cooper, A. F. (2014a). Ancient melt depletion overprinted by young carbonatitic metasomatism in the New Zealand lithospheric mantle. *Contributions to Mineralogy and Petrology*, 167(1), 963.
- Scott, J. M., Waight, T. E., van der Meer, Q. H. A., Palin, J. M., Cooper, A. F., & Münker, C. (2014b). Metasomatized ancient lithospheric mantle beneath the young Zealandia microcontinent and its role in HIMU-like intraplate magmatism. *Geochemistry, Geophysics, Geosystems*, 15(9), 3477-3501.
- Scott, J.M., Liu, J., Pearson, D.G., Harris, G.A., Czertowicz, T.A., Woodland, S.J., Riches, A.J.V. and Luth, R.W., 2019. Continent stabilisation by lateral accretion of subduction zone-processed depleted mantle residues; insights from Zealandia. *Earth and Planetary Science Letters*, 507, pp.175-186.
- Snow, J. E., & Dick, H. J. (1995). Pervasive magnesium loss by marine weathering of peridotite. *Geochimica et Cosmochimica Acta*, 59(20), 4219-4235.
- Shirey S.B., Walker R.J. 1998 -The Re-Os Isotope System in Cosmochemistry and High-Temperature Geochemistry. *Annual Review of Earth and Planetary Sciences*, 26, 423-500.

- Simon, N.S.C., Neumann, E.-R., Bonadiman, C., Coltorti, M., Delpech, G., Grégoire, M., Widom, E. 2008 - Ultra-refractory domains in the oceanic mantle lithosphere sampled as mantle xenoliths at ocean islands. *Journal of Petrology*, 49, 1223-1251.
- Stracke, A., Snow, J. E., Hellebrand, E., Von Der Handt, A., Bourdon, B., Birbaum, K., & Günther, D. (2011). Abyssal peridotite Hf isotopes identify extreme mantle depletion. *Earth and Planetary Science Letters*, 308(3-4), 359-368.
- Talbot, J.L., Hobbs, B.E., Wilshire, H.G., Sweatman, T.R. 1963 - Xenoliths and Xenocrysts from lavas of the Kerguelen archipelago. *American Mineralogist*, 48, 159-179.
- Taylor, W. R. (1998). An experimental test of some geothermometer and geobarometer formulations for upper mantle peridotites with application to the thermobarometry of fertile lherzolite and garnet websterite. *Neues Jahrbuch für Mineralogie-Abhandlungen*, 381-408.
- Valbracht, P.J., Honda, M., Matsumoto, T., Mattielli, N., McDougall, I., Ragettli, R., Weis, D. 1996 - Helium, neon, and argon systematics in Kerguelen ultramafic xenoliths: implications for mantle source signatures. *Earth and Planetary Science Letters*, 138, 29-38.
- van der Meer, Q. H., Scott, J. M., Serre, S. H., Whitehouse, M. J., Kristoffersen, M., Le Roux, P. J., & Pope, E. C. (2019). Low- $\delta^{18}\text{O}$ zircon xenocrysts in alkaline basalts; a window into the complex carbonatite-metasomatic history of the Zealandia lithospheric mantle. *Geochimica et Cosmochimica Acta*, 254, 21-39.
- Varne, R., Brown, A. V., & Falloon, T. (2000). Macquarie Island: its geology, structural history, and the timing and tectonic setting of its N-MORB to E-MORB magmatism. *Special Papers-Geological society of America*, 301-320.
- Walter, M.J., (1998). Melting of garnet peridotite and the origin of komatiite and depleted lithosphere. *Journal of Petrology*, 39, 29-60.
- Warren, J. M. (2016). Global variations in abyssal peridotite compositions. *Lithos*, 248, 193-219.

- Warren, J. M., Shimizu, N., Sakaguchi, C., Dick, H. J., & Nakamura, E. (2009). An assessment of upper mantle heterogeneity based on abyssal peridotite isotopic compositions. *Journal of Geophysical Research: Solid Earth*, 114(B12).
- Wasilewski B., Doucet L.S., Moine M., Beunon H., Delpech G., Mattielli N., Debaille V., Delacour A., Grégoire M., Guillaume D., Cottin J.-Y. 2017 - Ultra-refractory mantle within oceanic plateau: Petrology of the spinel harzburgites from Lac Michèle, Kerguelen Archipelago. *Lithos*, 272–273, 336–349
- Weaver, B. L., Wood, D. A., Tarney, J., & Joron, J. L. (1987). Geochemistry of ocean island basalts from the south Atlantic: Ascension, Bouvet, St. Helena, Gough and Tristan da Cunha. *Geological Society, London, Special Publications*, 30(1), 253-267.
- Weis D., Frey F.A., Leyrit H., Gautier I. (1993). Kerguelen Archipelago revisited: geochemical and isotopic study of the SE provinces lavas. *Earth and Planetary Science Letters*, 118, 101-119
- Weis, D., Shirey, S. B., Frey, F. A. 2000 - Re–Os systematics of Kerguelen plume basalts: enriched components and lower mantle source. *EOS Transactions, American Geophysical Union* 81, F1340.
- Wertz, K.L. (2003). From seafloor spreading to uplift: the structural and geochemical evolution of Macquarie Island on the Australian-Pacific Plate boundary. PhD Thesis, University of Texas. 189p.
- Witt-Eickschen, G., & Seck, H. A. (1991). Solubility of Ca and Al in orthopyroxene from spinel peridotite: an improved version of an empirical geothermometer. *Contributions to Mineralogy and Petrology*, 106(4), 431-439.
- Workman, R.K., & Hart, S.R, 2005. Major and trace element composition of the depleted MORB mantle (DMM). *Earth and Planetary Science Letters*, 231, 53-72.
- Yang H.J., Frey F.A., Weis D., Giret A., Pyle D., Michon G. 1998 - Petrogenesis of the flood basalts forming the northern Kerguelen archipelago: implications for the Kerguelen plume. *Journal of Petrology*, 39, 711-748.

- Zhang, X., Ganguly, J., & Ito, M. (2010). Ca–Mg diffusion in diopside: tracer and chemical inter-diffusion coefficients. *Contributions to Mineralogy and Petrology*, 159(2), 175.
- Zindler, A., & Hart, S. (1986). Chemical geodynamics, *Annual review of Earth and Planetary Sciences*, 14, 493-571.

ACCEPTED MANUSCRIPT

Figure captions

Figure 1. Map illustrating the Subantarctic and the tectonic plates and oceans within this area. Mantle xenoliths occur on the Auckland Islands, Crozet Island, Heard Island and Kerguelen. Abyssal peridotite outcrops on Macquarie Island, and has been dredged from the Southwest Indian Ridge and the America-Antarctica Ridge. Supra-subduction zone peridotite occurs on South Sandwich arc. AAR = America-Antarctica Ridge; SP = Sandwich Plate

Figure 2. Bathymetric map showing the Indian Ocean Subantarctic area and features discussed in the text. Red circles indicate locations of sites ODP (Ocean Drilling Project) 1137, 747 and 738 where material with continental crust affinities have been found (see text for details). The lower satellite image is of the Kerguelen archipelago with known peridotite xenolith occurrences after Wasilewski et al. (2017).

Figure 3. Major element compositions of minerals in Kerguelen peridotite xenoliths (data after Grégoire, 1994; Moine, 2000; Grégoire et al., 1997; 2000a-b; Moine et al., 2004; Delpech et al., 2004; Bascou et al., 2008; Wasilewski et al., 2017; Schiano et al., 1994; Hassler, 1999; this study). Ol; olivine, Cpx; clinopyroxene, Sp; spinel. $Mg\#(Ol, Cpx)$ and $Cr\#(Sp)$ are molar ratios of $100 \cdot Mg/(Mg+Fe^{2+})$ and $100 \cdot Cr/(Cr+Al)$. Indian abyssal cpx data from Dick & Bullen (1984) and Dick (1989). PUM = Primitive Upper Mantle estimates. Hydrous dunites contain hydrous minerals such as amphibole and/or phlogopite. Samples from this study are available in Supplementary Table 3. Carb-M samples refer to samples metasomatized by carbonatitic metasomatism (Delpech et al., 2004; Moine et al., 2004; Wasilewski et al., 2017). Error bars for some carbonate-rich samples show the extreme compositional major element variability in highly metasomatized samples. Spinel $Cr\#$ versus olivine $Mg\#$ and various fields updated plot from Scott et al. (2019).

Figure 4. Trace element and REE patterns of clinopyroxene in Kerguelen peridotite xenoliths. Data from Mattioli, 1994; Grégoire et al., 2000a-b; Mattioli et al., 1996; 1999; Moine et al., 2004; Delpech et al., 2004; Bascou et al., 2008; Wasilewski et al., 2017; Schiano et al., 1994; Hassler, 1999; this study). Samples from this study are reported in **Supplementary Table 3A**. Each REE spectrum is the average of several clinopyroxene (Cpx) core analyses, except a few individual analyses from Hassler (1999). Carb-M samples refer to samples metasomatized by carbonatitic metasomatism (Delpech et

al., 2004; Moine et al., 2004; Wasilewski et al., 2017). Melting curves are taken from Scott et al. (2016) and CI-Chondrite values from McDonough & Sun (1995).

Figure 5. Major element variations in bulk-rock peridotites xenoliths from the Kerguelen Islands (after Grégoire, 1994; Grégoire et al., 1997; 2000a; Moine et al., 2000; Hassler, 1999; this study). Samples from this study are available in Supplementary Table 3. Carb-M Lac Michèle harzburgites refer to samples metasomatized by carbonatitic metasomatism (Delpech et al., 2004; Wasilewski et al., 2017). PM estimate from McDonough and Sun (1995) and DMM estimate from Workman et al. (2005). Grey field; Horoman peridotites (Takazawa et al., 2000). Continuous black lines are residues of polybaric fractional melting at 2–0, 3–0, 5–1 and 7–2 GPa (Herzberg, 2004); thick dashed black lines correspond to 30 and 38% of polybaric fractional melting. Abyssal (n=446) and cratonic (n=250) peridotite density contours from Wasilewski et al. (2017). Siberian cratonic peridotites are fertile off-craton garnet and spinel peridotite xenoliths from central Asia (see Wasilewski et al., 2017 for details). Average for OI1-u bulk peridotites (ultra-refractory oceanic island peridotites) from Simon et al. (2008).

Figure 6 : Present-day Sr-Nd isotopic compositions for the Kerguelen xenolith suite. Analyses correspond either to bulk-rock or clinopyroxene separates (Mattielli et al., 1996, 1999; Hassler, 1999). The fields for Kerguelen type-II xenoliths (granulites) is from Mattielli et al. (1996, 1999) and Hassler (1999). Fields for Kerguelen and Heard volcanic rocks and ODP LEG 183 (site 1137-Elan Bank), 120 (site 747) and 119 (site 738) after <http://georoc.mpch-mainz.gwdg.de/georoc/>. Fields for sites 1137, 747 and 738 indicate plume-derived Cretaceous Kerguelen plateau volcanics with trace element and isotopic compositions indicative of contamination by continental lithosphere derived-magmas, these geochemical fingerprints have not yet been found in Kerguelen Islands basalts. Acronyms: MORB; Mid Ocean Ridge Basalt; SEIR MORB; South East Indian Ridge MORB; HIMU; High μ (high time-integrated U/Pb material); EM I and EM II are Enriched Mantle components I and II, BSE; Bulk Silicate Earth, see Zindler & Hart (1986) for details.

Figure 7. Bathymetric map showing the Southern Ocean Subantarctic and features discussed in the text.

Figure 8. Auckland Island peridotite equilibration temperatures, projected onto the 70 mWm⁻² geotherm of Hasterock and Chapman (2011). The spinel-garnet transition is for Iherzolite (Klemme and O'Neil 2000) and a more Cr-rich bulk composition would increase the P of the transition. The column on the right indicates the inferred lithosphere thickness underneath the Auckland Islands at the Miocene time of xenolith entrainment.

Figure 19. Auckland Island Type 1 (**9A**) and Type 2 (**9B**) and Macquarie Island (**9C**) peridotite clinopyroxene REE data plotted against theoretical clinopyroxene compositions for different percentages of bulk peridotite melting. Auckland Island data are from Scott et al. (2014b) and Macquarie Island are from Dijkstra et al. (2010). Theoretical clinopyroxene compositions are from Scott et al. (2016). CI chondrite is from Sun and McDonough (1989).

Figure 10. Summaries of T_{RD} ages for Subantarctic mantle peridotites. 10A. Histograms for different locations. B. Auckland Island and Macquarie Island osmium versus bulk rock Al₂O₃ and/or Pd/Ir. The Zealandia data are from McCoy-West et al. (2013), Liu et al. (2013) and Scott et al. (2019); the Kerguelen data are from Hassler (1998) and Hassler and Shimuzu (1998); the Dun Mountain Ophiolite Belt (OB) data are from Scott et al. (2019); Macquarie Island data are from Dijkstra et al. (2010); and the abyssal peridotite data are from Day et al. (2017). PUM; Primitive Upper Mantle value from Meisel et al. (2001).

Figure 11. South Atlantic Ocean Subantarctic features, with locations of mantle samples. Bathymetric depth decreases from red to green. Blue circles on the South Sandwich arc indicate locations of dredged and drilled peridotite (Pearse et al. 2001).

Table 1. Summary of Subantarctic Islands and mantle occurrences.

Subantarctic Island Group	Ocean	Latitude	Area (km ²)	Administrator	Mantle peridotite xenoliths?
South Georgia and South Sandwich	Atlantic	54°S	3903	Britain	No, but peridotite dredged and drilled
Bouvet	Atlantic	54°S	49	Norwegian	No
Heard and McDonald	Indian	53°S	368	Australia	Yes , but only on Heard Island. (S. O'Reilly unpublished data)
Crozet	Indian	46°S	352	French	No. Dunites reported are cumulates
Kerguelen	Indian	49°S	7215	French	Yes
Prince Edward and Marion	Indian	46°S	335	South Africa	No
Macquarie	Southern	55°S	128	Australia	No, but exhumed oceanic mantle
Antipodes	Southern	49°S	21	New Zealand	No
Auckland	Southern	51°S	626	New Zealand	Yes
Bounty	Southern	47°S	1.4	New Zealand	No
Campbell	Southern	52°S	113	New Zealand	No
Snares	Southern	48°S	3.5	New Zealand	No

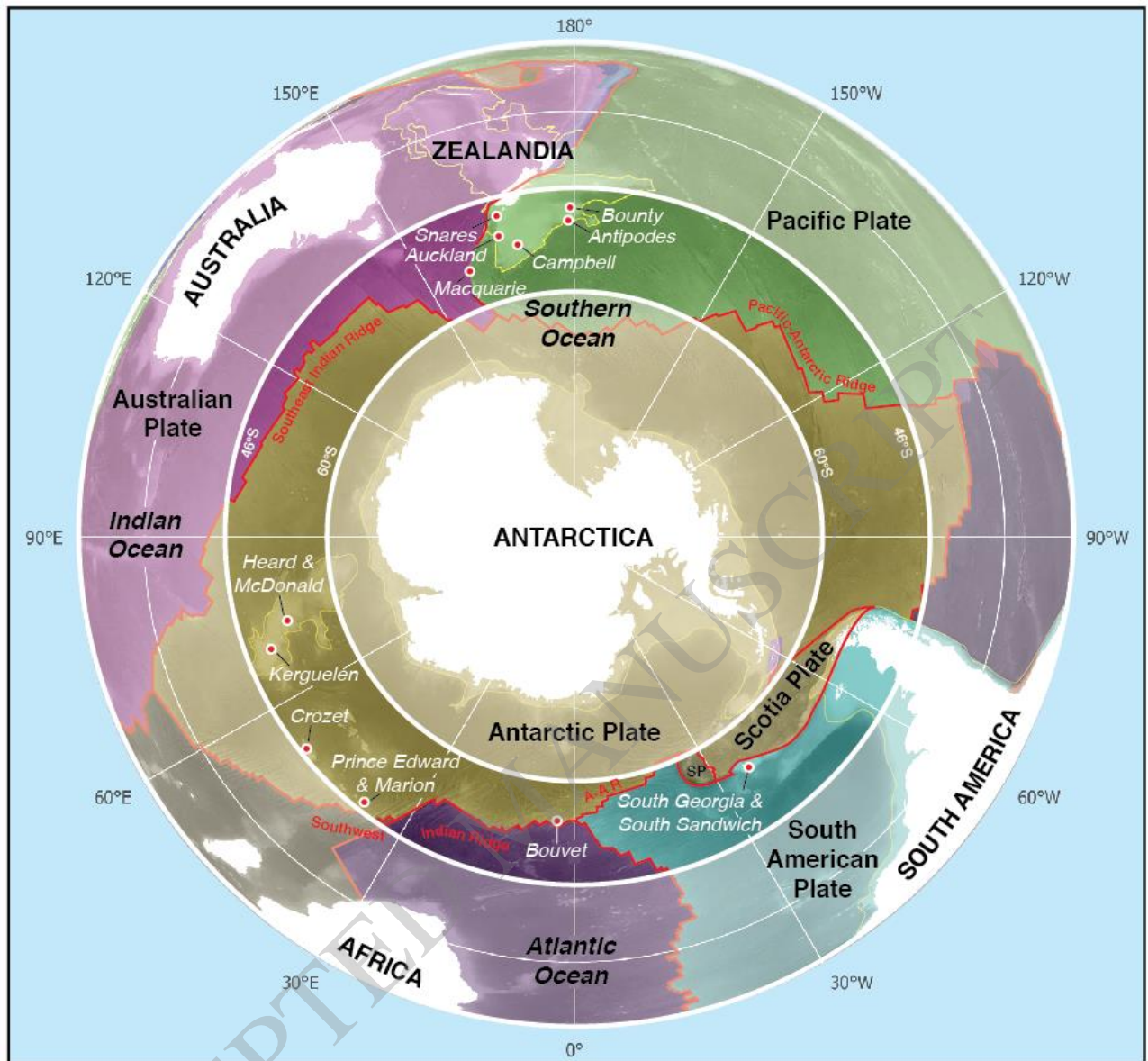


Figure 1

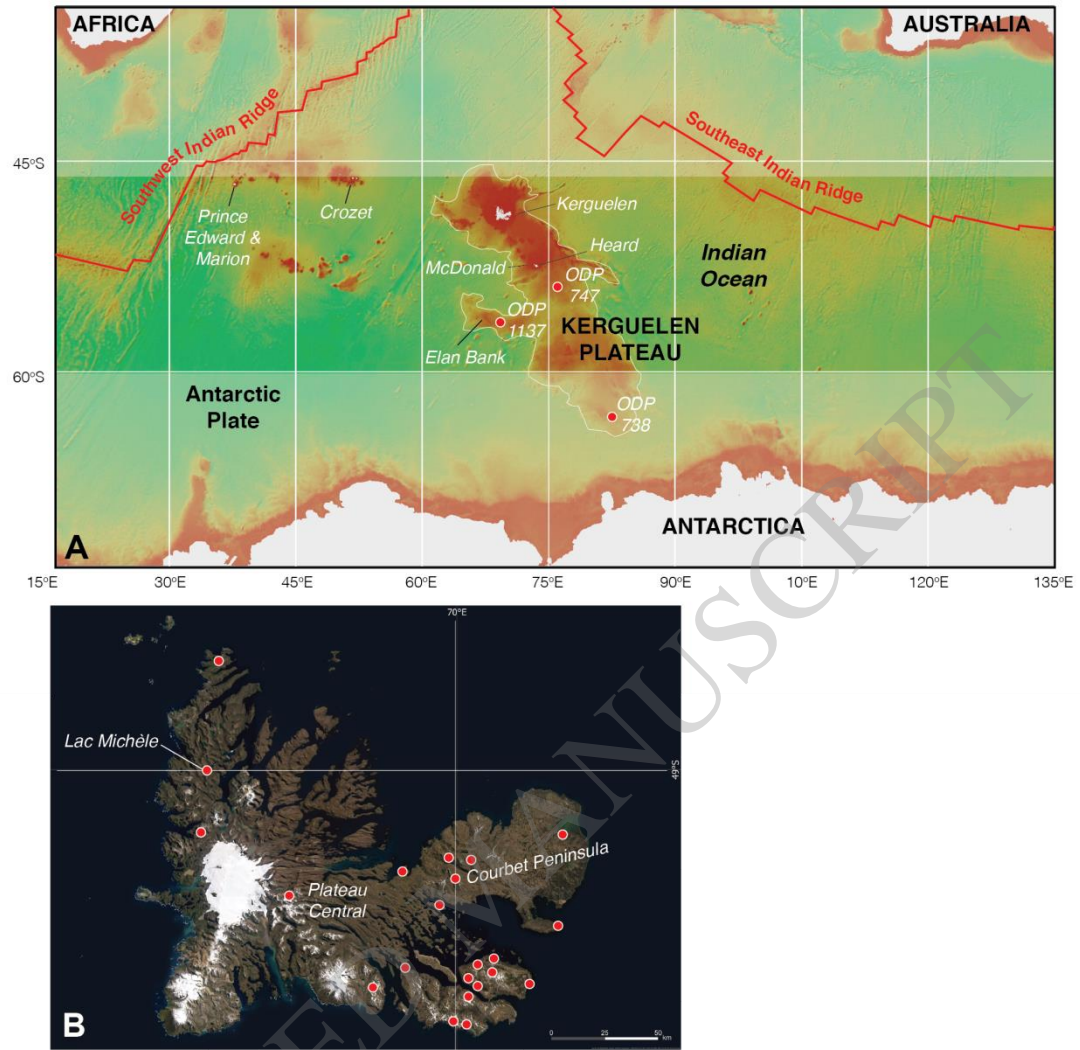


Figure 2

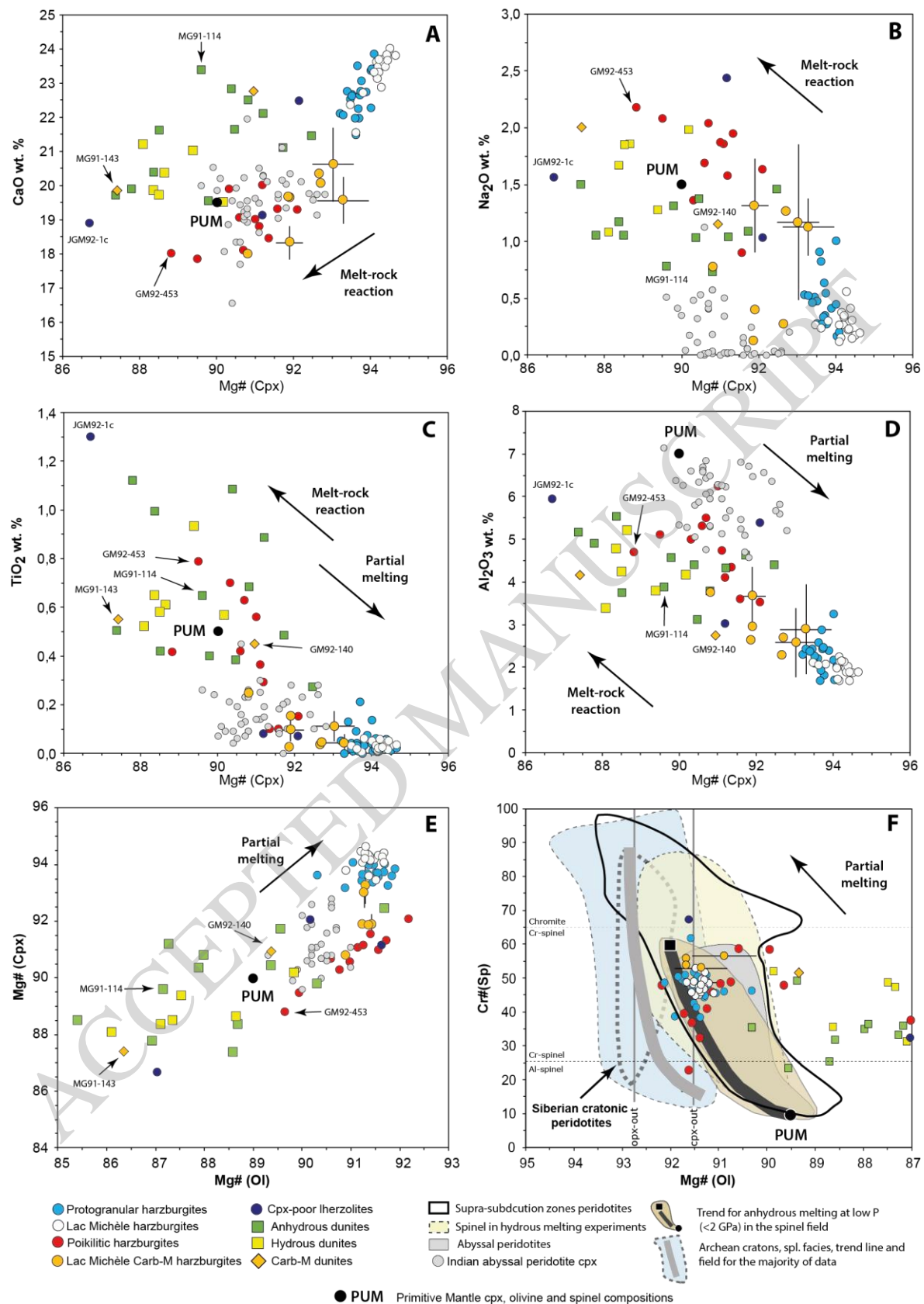


Figure 3

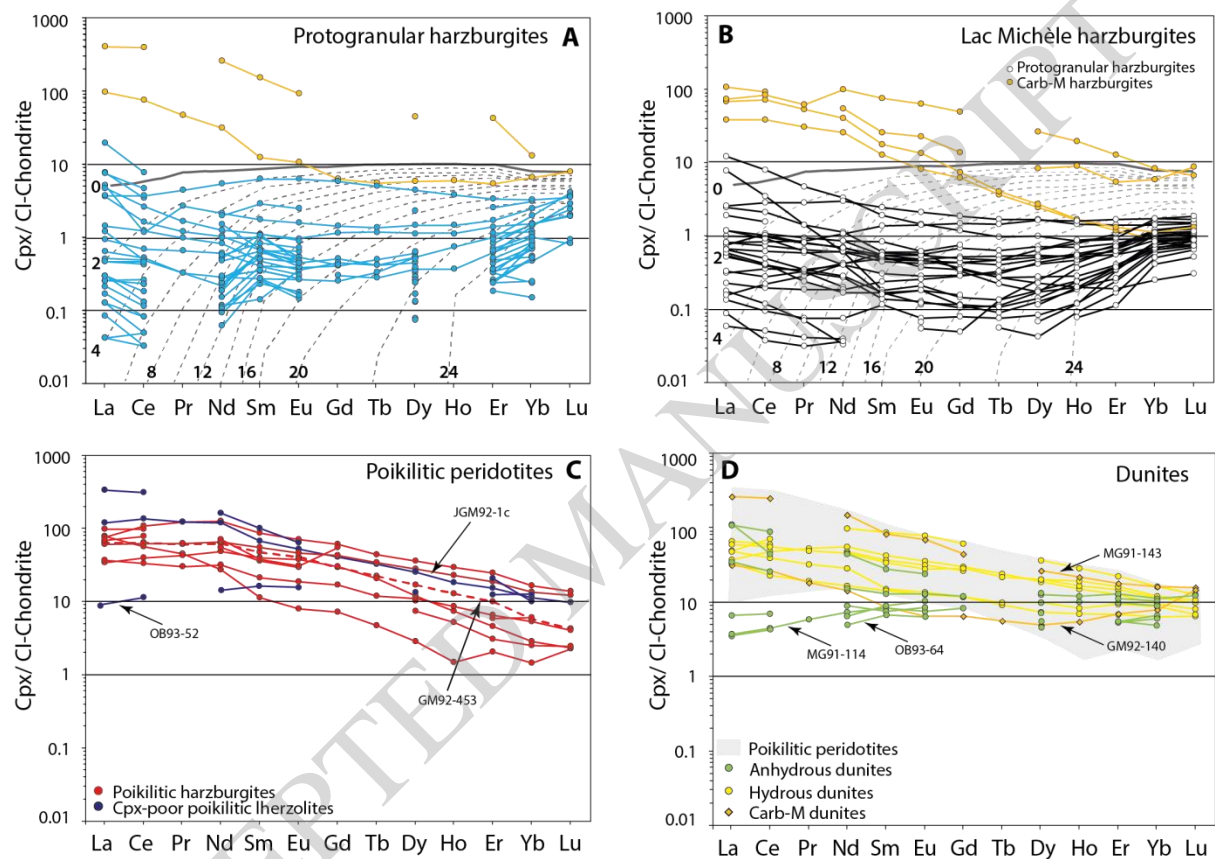


Figure 4

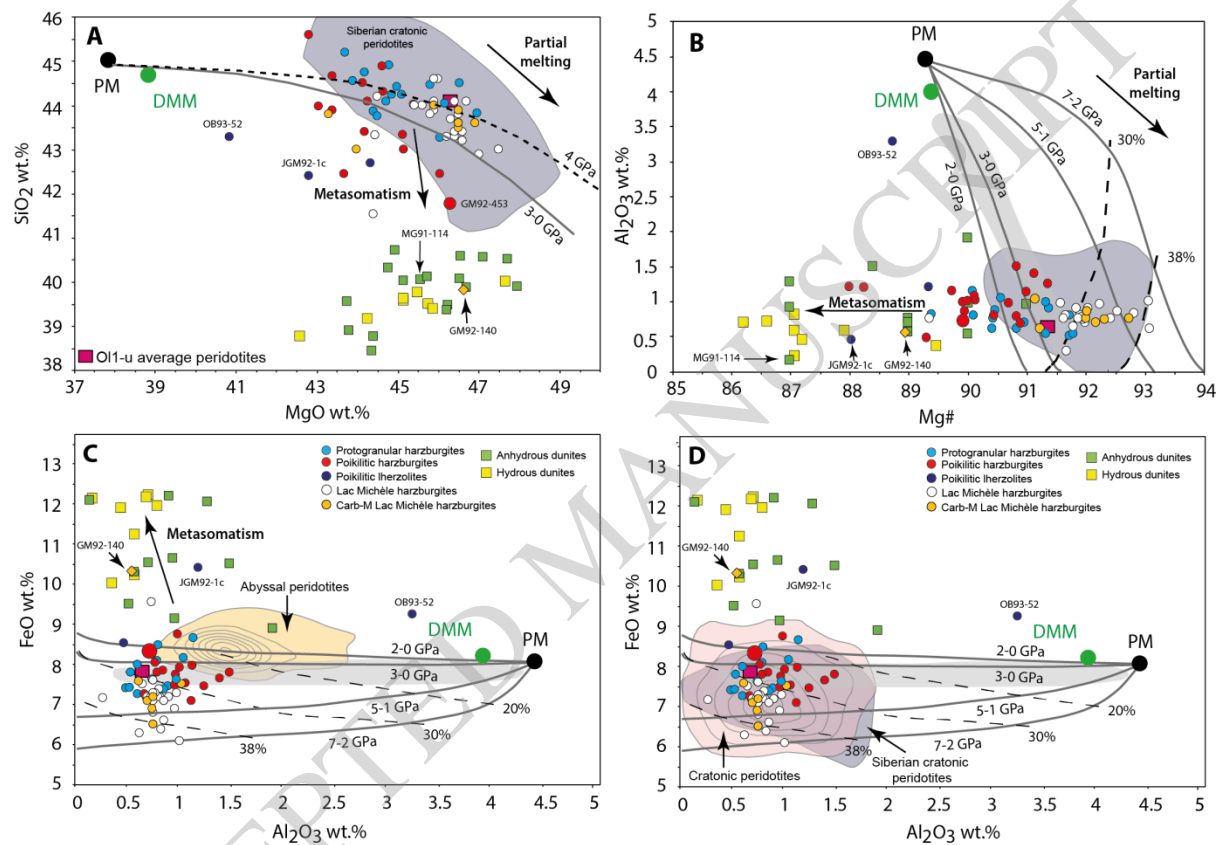


Figure 5

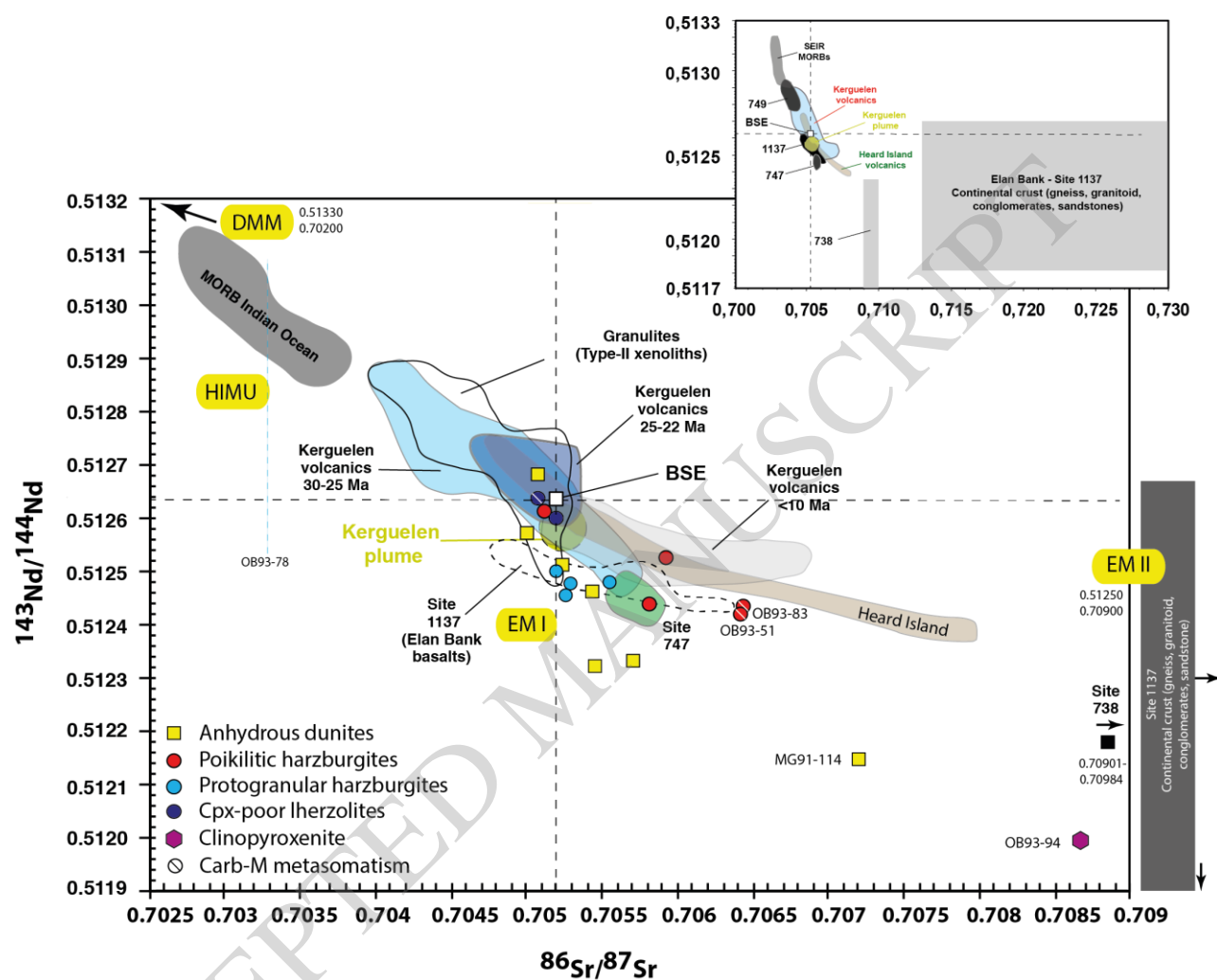


Figure 6

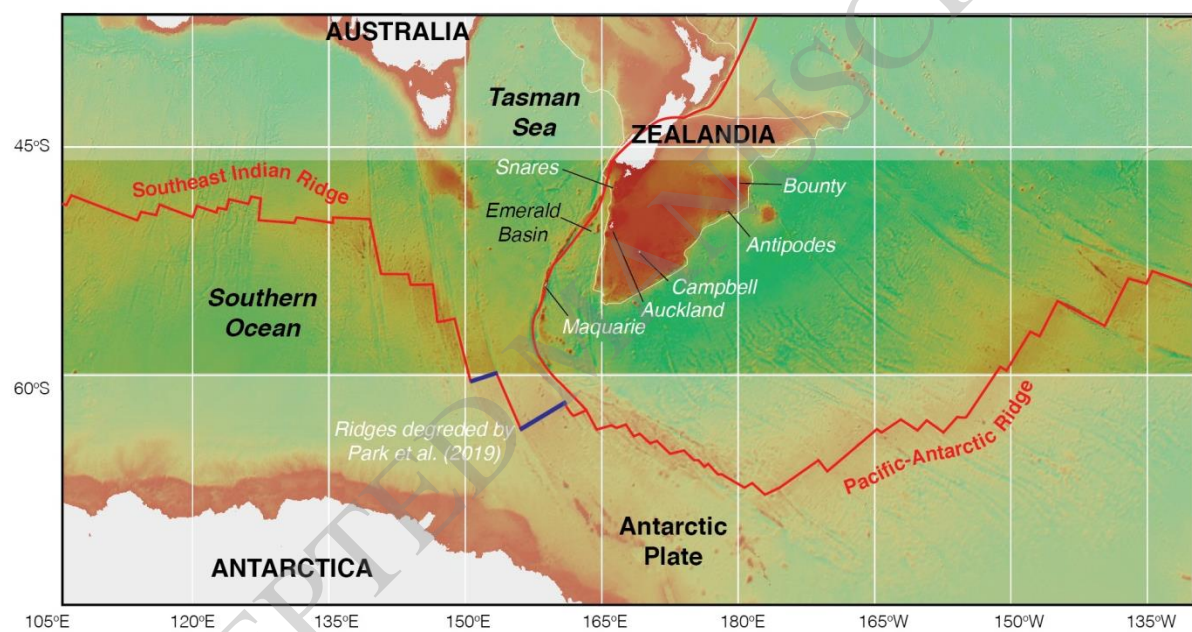


Figure 7

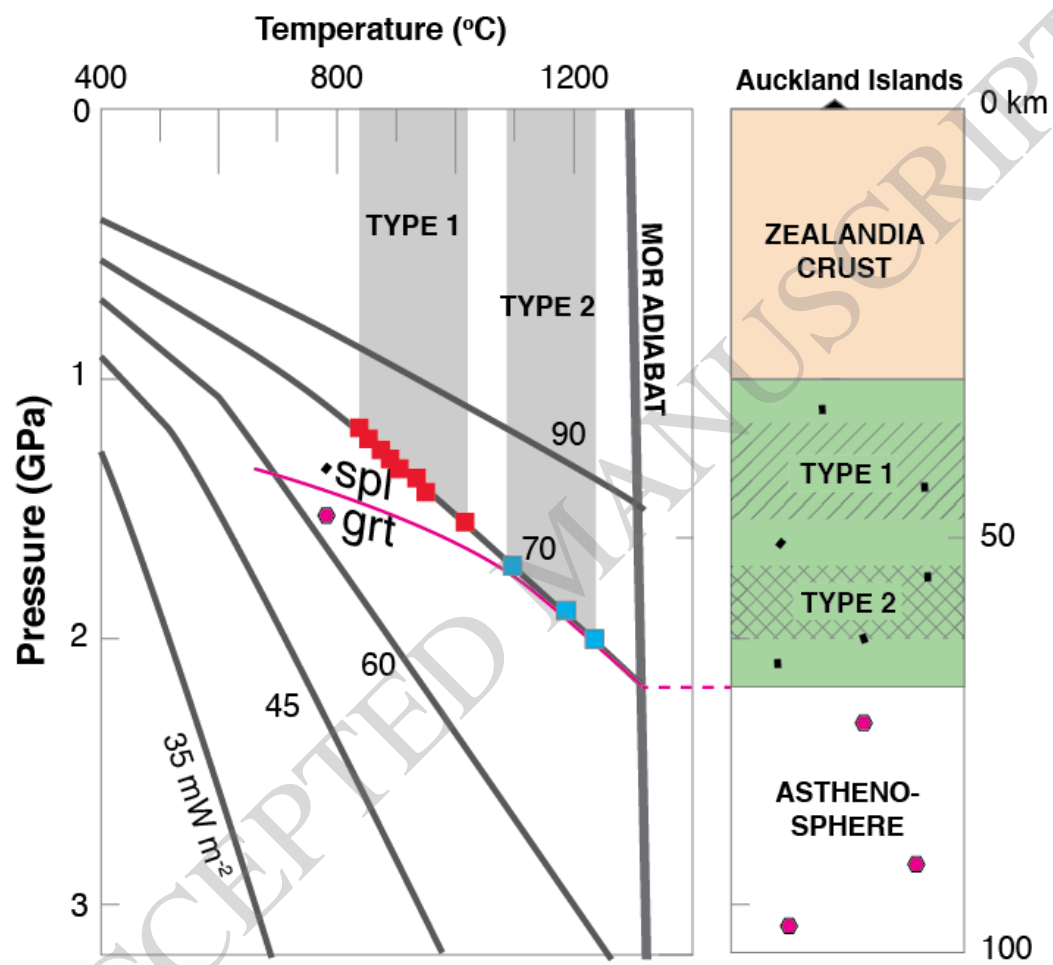


Figure 8

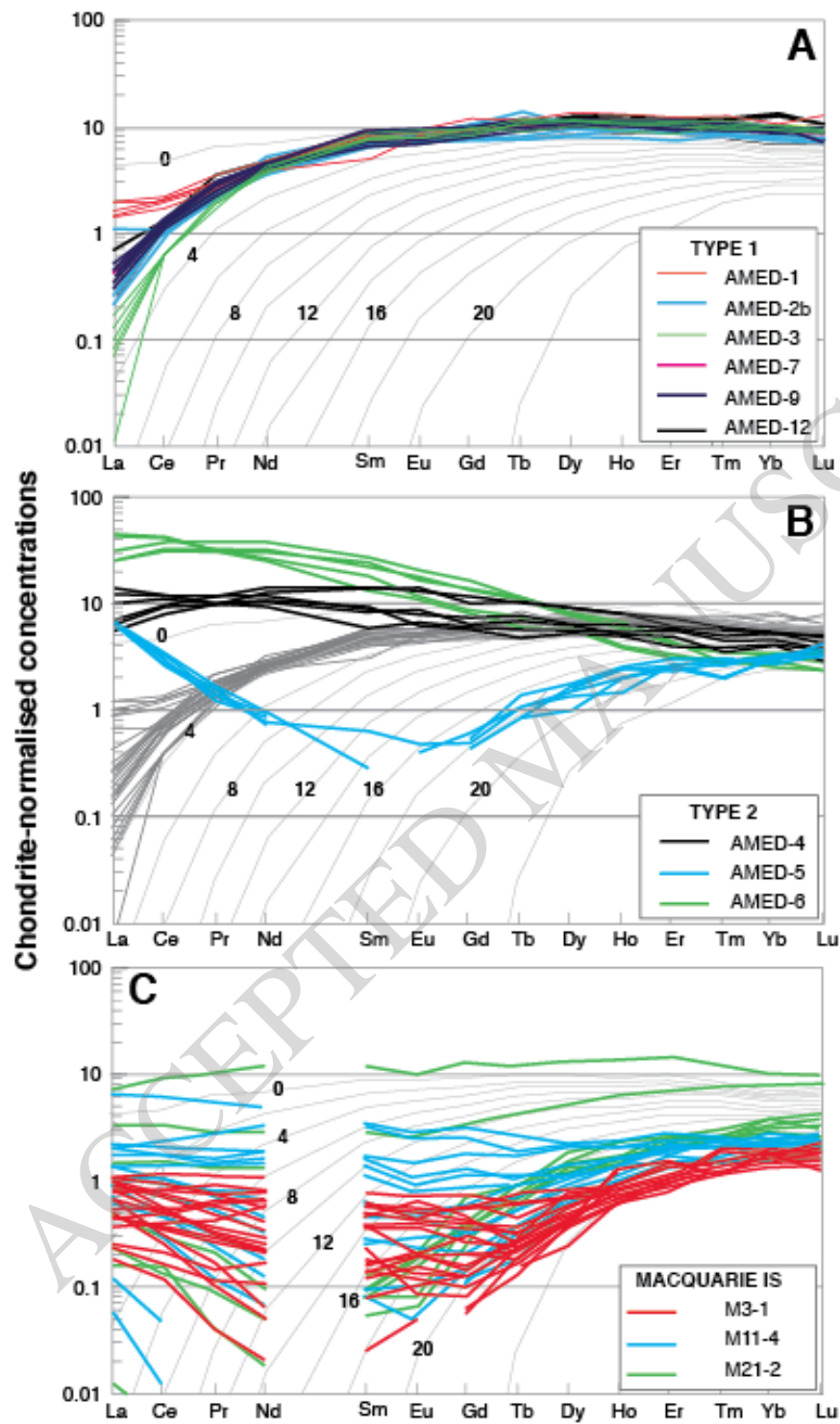


Figure 9

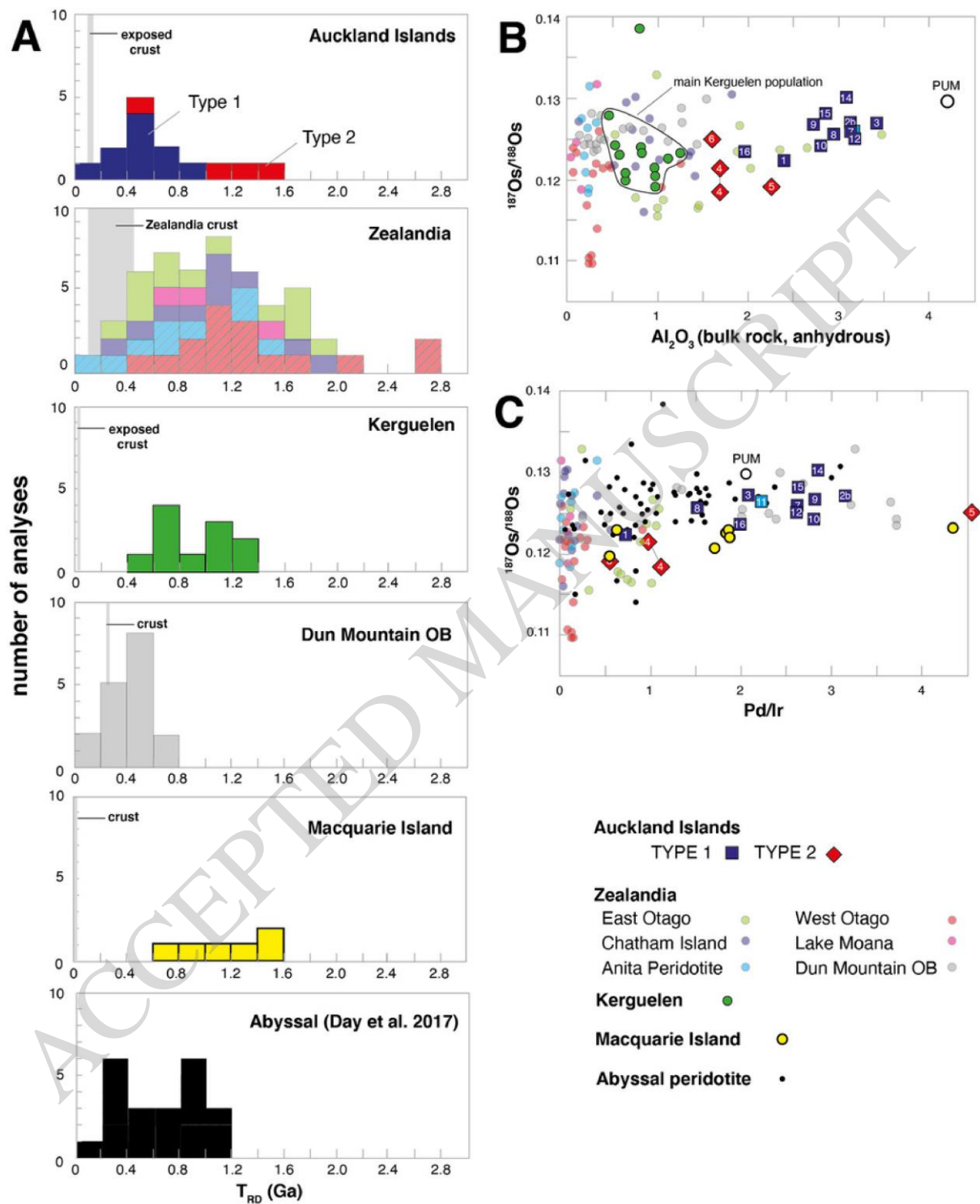


Figure 10

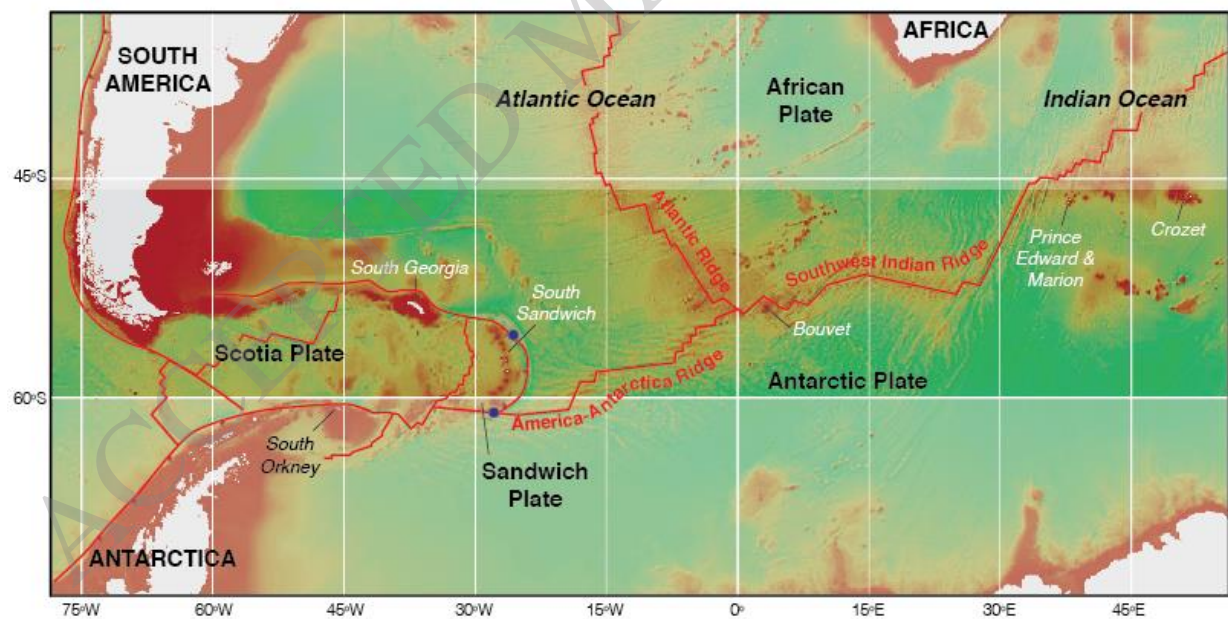


Figure 11